The Granular Origins of Tail Risk in the Cross-Section of Asset Prices

PRELIMINARY DRAFT

Torben G. Andersen* Yi Ding† Viktor Todorov‡

July 5, 2024

Abstract

We study the tail dispersion risk in the cross-section of asset prices at high frequencies. We show that the cross-sectional tail behavior of asset returns depends on whether the price increment contains a systematic jump event or not. In case of systematic jumps, the cross-sectional asset return tail behavior is determined by the assets' exposures to the systematic event, while if the interval contains no systematic jump, it is determined by the tails of the idiosyncratic jumps. We develop an estimator for the tail shape of the cross-sectional asset return distribution with distinct asymptotic properties, depending on whether the interval contains a systematic jump or not. We show empirically that shocks to the tail shape parameters of the cross-sectional asset return distribution are source of priced risk. The price of this tail dispersion risk depends on its source: fat idiosyncratic tails are liked by investors and carry negative premiums, while fat tails in assets' exposures to systematic jumps are disliked and carry positive premiums.

*Finance Department, Kellogg School of Management, Northwestern University. Email: t-andersen@kellogg.northwestern.edu.

†Faculty of Business Administration, University of Macau, Macau. Email: yiding@um.edu.mo.

‡Finance Department, Kellogg School of Management, Northwestern University. Email: v-todorov@kellogg.northwestern.edu.

1 Introduction

Tail risk in asset returns plays an important role in financial economics. In particular, there is extensive evidence showing that investors demand compensation for bearing tail risk. Our objective is to study a tail dispersion risk in the cross-section of asset prices at high frequencies. The focus on high-frequency returns allows us to establish, in a model-free (nonparametric) way, a connection between the tail risk dispersion of the assets and the underlying features of the assets' return dynamics. More specifically, we show that the tail behavior of the cross-sectional asset return distribution differs depending on whether the time interval contains a systematic jump event or not. The latter is defined as a jump that has a pervasive effect on the entire cross-section of asset prices, i.e., it affects a nontrivial fraction of the stocks. Examples of systematic jumps are times when the market portfolio jumps or, more generally, when systematic risk factors affecting the returns exhibit a jump.[1] When a systematic jump is present within a short time interval, the tails of the cross-sectional return distribution are governed by the assets' exposure to that jump risk. When this is not the case, the tails of the cross-sectional return distribution are determined by the tail properties of the idiosyncratic jump risk in asset prices. In contrast, if we were to consider returns over coarser time intervals, the cross-sectional tail behavior will be governed by the mixture of these two sources of tail risk as well as the properties of the time-varying asset volatility. The use of high-frequency data, therefore, is critical for us in disentangling the different sources of tail risk in asset prices.

We develop inference tools for assessing the cross-sectional tail dispersion risk in asset prices at high frequencies. Specifically, assuming that the cross-sectional return tails obey an approximate power law, we characterize the tail behavior via two parameters only - the scale and shape of the tails. We propose non-parametric estimators of these tail shape parameters using a large cross-section of asset returns. The es-

[1] While many systematic jumps can be connected with observable factors, Jacod et al. (2024) show that the cross-section of asset returns often is exposed to such systematic events that are not readily connected to jumps in observable factors.

timators have different asymptotic behavior depending on whether the time interval contains a systematic jump or not. The reason is the very different manifestation of idiosyncratic and systematic jumps in the high-frequency data. On the one hand, estimating the tail behavior from exposure to systematic jumps is infeasible unless they occur within our high-frequency intervals. On the other hand, whenever such a jump occurs, a nontrivial fraction of the assets jump and can be used for estimating the tails. In contrast, the likelihood of an idiosyncratic jump is proportional to the length of the interval, which shrinks asymptotically in our setting. Nonetheless, for this scenario, we can exploit a string of consecutive time intervals for estimation, which is not possible for systematic jumps because they, by definition, are rare events that materialize only at distinct instances. We establish asymptotic normality of our tail estimators under the condition that both the number of stocks and the sampling frequency diverge. We also propose a goodness-of-fit test for the power law in the tails based on a Kolmogorov-Smirnov (KS) statistic.

Implementing our inference procedures, the goodness-of-fit test suggests that the power law provides a good approximation to the tail features of the cross-sectional asset return distributions for the S&P 500 equity index constituents at the 10-minute frequency between 2003 and 2022. We further find nontrivial variation in the time series of the tail shape indices over the sample period. Moreover, the time-series variation in the tail shape indices of systematic and idiosyncratic jumps differ, and their dynamics are distinct from that of the market volatility as well as the common idiosyncratic volatility (i.e., the cross-sectional average of idiosyncratic volatility).

These differences in time-series behavior imply that shocks to the tail shape parameter of the cross-sectional high-frequency return distribution may constitute a distinct source of systematic risk that is of concern to investors. We investigate this hypothesis through formal asset pricing tests. For this analysis, we use daily returns for the universe of all traded stocks between 2004 and 2022, except for the exclusion of micro-cap and penny stocks, following common practice in the literature. Hence, we enlarge the cross-section in the asset pricing test significantly relative to the one used for constructing the tail shape indices, with the latter requiring returns that are robust to market microstructure frictions. Our interest is whether innovations (shocks) to the tail shape indices are priced sources of risk. Towards this end, we

estimate the assets' exposure towards these shocks using daily returns and our daily time series of tail shape indices. We then implement a classic sorting exercise on the tail shape betas and check if the generated spread of the high-minus-low portfolios can be rationalized with exposures to existing systematic factors.

We find that stocks with high exposure to positive shocks to the systematic jump tail shape, i.e., stocks that perform relatively well when the tails fatten, have low future returns. The return spread between the Low and High quintile portfolios is economically large and remains statistically significant after controlling for a number of systematic risk factors including the Market, Fama-French three/five/six factors (FF3/FF5/FF6, Fama and French (1993, 2015, 2018)), the tail risk factor by Kelly and Jiang (2014), the idiosyncratic risk factor of Ang et al. (2006)), and the common idiosyncratic volatility factor of Herskovic et al. (2016). The portfolio performance is robust to different weighting schemes (equal/value weight) and portfolio holding windows (one/three months). The results suggest that investors dislike fat tails in the distribution of assets' exposure to systematic jumps and, vice versa, favor thin tails. Economically, it implies that periods of elevated cross-sectional dispersion at systematic jump events are viewed as bad scenarios and hedging them requires a risk premium in equilibrium. Of course, this is also consistent with the standard view that investors are averse to increased return dispersion induced by systematic risk.

In contrast, our analysis reveals a striking and significant reversal in the sign of the risk premium when we consider shocks to the tail shape index of the idiosyncratic jumps. These tail shocks are also priced, but the price of risk is now negative. That is, investors react favorably to a fattening of the idiosyncratic jump tails in asset returns. The return spread between the High and Low quintile portfolios sorted on the idiosyncratic tail shape betas is positive and statistically significant after controlling for our set of common risk factors. These portfolio sorting results are robust to both the equal/value weighting schemes and portfolio holding window (one/three months). This finding is harder to rationalize within standard economic models in which higher volatility and/or jump risk typically is disliked by investors. However, this type of result has been obtained in a number of prior studies, and the usual explanation is behavioral - investors seem to have an element of lottery-like preferences, as documented in equity and option market settings by, e.g., Boyer and Vorkink (2014); Blau

et al. (2016) and Filippou et al. (2018). Prior theoretical research has also explored the modeling of lottery-like preferences and their pricing implications; for example, the optimal belief model by Brunnermeier et al. (2007) and the cumulative prospect theory by Barberis and Huang (2008).

The finding of a significant premium for tail shape risk that changes sign - depending on whether the return dispersion stems from systematic or idiosyncratic jumps - demonstrates the necessity of treating price increments with and without systematic jumps differently. A natural question is whether these tail shape risks are related? We find that there is a very weak correlation between the shocks and between the high-versus-low portfolios sorted on the different tail-shape betas. Consequently, the economic mechanisms explaining these pricing effects differ, as already alluded to above. From a practical point of view, this implies that one can obtain even stronger performance by exploiting these pricing effects jointly. Towards this end, we construct a simple equally-weighted portfolio with the two sorted portfolios, namely, the HmL portfolio sorted on idiosyncratic jump tail shape shock betas and the LmH portfolio sorted on systematic jump tail shape shock betas. The combined portfolio has zero-net cost and achieves additional diversification through the weighting scheme. We show this portfolio, as hypothesized, delivers a higher Sharpe ratio than the two individual tail-risk sorted portfolios.

Related Literature

Our study is situated within a broader literature that explores the power-law tail behavior of various economic and financial variables. Power-law tail patterns have been observed in domains ranging from city sizes (Kingsley Zipf (1932); Gabaix (1999); Eeckhout (2004)), income distributions of companies (Okuyama et al. (1999)), firm sizes (Axtell (2001)), macroeconomic disasters (Barro and Jin (2011)), and stock trading volume (Gopikrishnan et al. (2000)). These studies find that power-law tail behavior is crucial for comprehending key mechanisms in economics and finance like the source of aggregate economic fluctuations. For example, Gabaix et al. (2003, 2006) argue that heavy-tailed financial returns and the stock market crashes can be explained by concentrated trades by large market participants. The heavy-tailedness

in firm sizes is used to explain the aggregate economic movements in the US market (Gabaix (2011)) and the international market (Di Giovanni and Levchenko (2012)). Acemoglu et al. (2012, 2017) show that when there exist fat-tailed inter-sectoral input-output linkages, micro-economic idiosyncratic shocks may lead to sizable aggregate fluctuation and systematic macroeconomic tail risks.

Our paper is closely related to studies exploring the power-law behavior of stock returns. Financial returns are known to conform to a heavy-tailed distribution that can be accommodated by a Pareto distribution; see, e.g., Mandelbrot (1963); Fama (1965); Gopikrishnan et al. (1999); Gabaix (2012). Bollerslev and Todorov (2011) propose a non-parametric estimator of tail-shape risk, which is the tail-shape parameter of the power law based on high-frequency data of univariate processes. Notably, substantial time-variation and serial dependence is found in the market tail-risk index by Bollerslev and Todorov (2011) and Bollerslev et al. (2015), with the latter using option data for estimation. Unlike these studies, our focus is on the cross-sectional tail behavior in a large number of assets and its implications for asset prices.

Our focus on the tails of the cross-sectional asset return distribution is similar to that of Kelly and Jiang (2014), who study the time-varying cross-sectional tail risk estimated from daily data. They find empirically that the daily tail shape index can be used in stock return prediction. Different from Kelly and Jiang (2014), we investigate the cross-sectional tail behavior of returns at high frequencies. We find that this behavior differs both from a statistical and economic point of view depending on whether the time interval contains a systematic jump event or not. In that sense, we explore the granular origin of cross-sectional tail dispersion risk in asset prices.

Finally, our work is closely connected to the general literature on tail risk and time-varying volatility risk, as well as their effect on the cross-section of asset prices. The literature on tail risk and asset pricing is extensive. Jump tail risk, and in particular the left jump tail, is shown to be helpful in predicting future returns in the U.S. market (Bollerslev et al. (2015); Andersen et al. (2015)) and internationally (Andersen et al. (2020, 2021). Lin and Todorov (2019) find that aggregate idiosyncratic asymmetric jump variations predict future equity returns. Several studies show that tail risks help explain the cross-section of asset returns. Cremers et al. (2015) find that stocks with high exposure to aggregate jump risk have contemporaneous high expected returns

in the cross-section. Bollerslev et al. (2016) show that jump betas entail significant risk premiums. Bollerslev et al. (2020) find stocks with high positive-minus-negative jump volatilities have high returns. Ang et al. (2006) find that stocks with low (idiosyncratic) volatilities have high positive returns. Bali et al. (2011) explain the puzzling effect of idiosyncratic risk using lottery-like preferences and find that stocks with historically high maximum returns are overpriced and have low future returns in the cross-section. Herskovic et al. (2016) evaluate the aggregated idiosyncratic risk and find that shocks to the common idiosyncratic volatility (CiV) are negatively priced. We contribute to this strand of the literature by examining the distinct pricing implications of shocks to the tail shape of the cross-sectional asset return distribution stemming from systematic versus idiosyncratic high-frequency jumps.

Outline

The remainder of the paper is organized as follows. Section 2 introduces our model setup and states the assumptions. Section 3 presents our theoretical inference results. Section 4 contains a Monte Carlo study. We assess empirically the cross-sectional asset return tail dispersion risk in Section 5. Asset pricing implications of cross-sectional asset tail risk variation are provided in Section 6. All proofs and additional mathematical details and empirical results are collected in Appendices A–G.

2 Setup

We denote the log-price of an asset i at time t with p_{it} for $i = 1, ..., N$. It has the following general dynamics:

$$p_{it} = p_{i0} + \int_0^t \alpha_{is} ds + \int_0^t \boldsymbol{\beta}_{i,s}^\top d\mathbf{W}_s + \int_0^t \widetilde{\sigma}_{is} d\widetilde{W}_{is} + J_{it} + \widetilde{J}_{it}, \tag{2.1}$$

where $\mathbf{W}_t = (W_t^1, ..., W_t^k)^\top$, for some positive integer k and $W_t^1, ..., W_t^k$, $\widetilde{W}_{1t}$,..., $\widetilde{W}_{Nt}$ are independent standard Brownian motions, J_{it} and $\widetilde{J}_{it}$ are the systematic and idiosyncratic respectively jump components of the asset prices. The formal definition of these processes is given in Appendix D. On an intuitive level, however, the difference

between systematic and idiosyncratic jumps is clear: the former are pervasive in the sense that they arrive together and impact a nontrivial fraction of the cross-section of asset prices, while the latter arrive independently. Our setup is very general and does not involve any assumption regarding the source of risk driving the systematic jumps, i.e., we do no link the systematic jumps to jumps of observable systematic risk factors. Similarly, we do not make an assumption about the source of systematic diffusive risk. This is an important generality of our setup given the large number of alternative systematic factors put forth in the asset pricing literature.

As we will see later, the cross-sectional tail behavior of asset prices at high frequencies depends critically on whether the given interval contains a systematic jump or not. The timing of systematic jumps can be consistently estimated using the method of Jacod et al. (2024). We assume that this identification of systematic jump locations has been performed, and we state this as a high-level assumption.

Towards this end, suppose we sample the asset prices over the fixed interval $[0,1]$ at equidistant times $0, 1/n, 2/n, ..., 1$ and denote the length of the sampling interval by $\Delta_n = 1/n$ and the log-price increment by $\Delta_j^n p_i = p_{i,j\Delta_n} - p_{i,(j-1)\Delta_n}$, for $j = 1, ..., n$. Let us denote with T_n the set of indices of the high-frequency increments containing the systematic jumps and with $\widehat{T}_n$ an estimator of this set. Formal definitions of T_n and $\widehat{T}_n$ are given in Appendix D. In our application we will use the method of systematic jump identification given in Jacod et al. (2024). Our tail inference will be performed separately on $\widehat{T}_n$ and its compliment set $\widehat{T}_n^c$, i.e., on the set of increments with and without detected systematic jumps.

We focus on the cross-sectional tail behavior of high-frequency returns which, in turn, is linked to the tail behavior of systematic and idiosyncratic jumps in asset prices. The tail dispersion risk can vary over time in a stochastic way and we will assume that this variation is adapted to the σ-algebra $\mathcal{C}$ of "common shocks," which contains various aggregate level shocks. Intuitively, $\mathcal{C}$ captures everything that is related to systematic risk in the economy.

We will assume that the tails of the large jumps have regular variation. Similar to Bollerslev and Todorov (2011), this assumption is formulated in terms of jumps in the asset price level (recall that p_{it} denotes the log-price). More specifically, we define

$\psi(x) = \exp(|x|) - 1$, and let

$$\psi^+(x) := \begin{cases} \psi(x), & x > 0, \\ 0, & x \leq 0, \end{cases} \qquad \psi^-(x) := \begin{cases} 0, & x > 0, \\ \psi(x), & x \leq 0. \end{cases}$$

For a generic function $g : \mathbb{R} \to \mathbb{R}$, we then denote $g^{\pm}_{\psi}(x) = \frac{g(\pm \log(1+x))}{1+x}$, and the tail of the measure $g^{\pm}_{\psi}(x)$ by

$$\overline{g}^{\pm}_{\psi}(x) := \int_x^{\infty} g^{\pm}_{\psi}(u)du,$$

for some $x > 0$.

Conditional on $\mathcal{C}$, the systematic jumps in the asset prices are assumed to be identically and independently distributed in the cross-section at each jump time p, with conditional jump distribution given by $f_p(x)$. We assume regular variation for $f_p(x)$. That is,

$$\frac{\overline{f}^{\pm}_{p,\psi}(x+u)}{\overline{f}^{\pm}_{p,\psi}(x)} \approx \left(1 + \frac{u}{x}\right)^{-1/\xi^{\pm}_S}, \quad \text{as } x, u \to +\infty \text{ with } u \geq 0, \tag{2.2}$$

for some tail shape parameters $\xi^{\pm}_S$, which are $\mathcal{C}$-adapted random variables. We make this approximation formal in Appendix D. Our assumption of an i.i.d. jump size distributions in the cross-section, conditional on $\mathcal{C}$, is natural if we think of the available stocks as being drawn randomly from a population with an infinite set of assets, corresponding to our asymptotic scheme, where N is diverging, see, e.g., Gagliardini et al. (2016) for a detailed discussion of this perspective.

We make a similar regular variation assumption for the idiosyncratic jumps. Specifically, letting $\nu_{t,i}(x)$ denote the time-varying jump intensity of $\widetilde{J}_{it}$, we assume,

$$\frac{\overline{\nu}^{\pm}_{t,i,\psi}(x+u)}{\overline{\nu}^{\pm}_{t,i,\psi}(x)} \approx \left(1 + \frac{u}{x}\right)^{-1/\xi^{\pm}_I}, \quad \text{as } x, u \to +\infty \text{ with } u \geq 0, \tag{2.3}$$

for some tail shape parameters $\xi^{\pm}_I$, which are $\mathcal{C}$-adapted random variables.

3 Inference for asset return tails at high frequencies

We proceed with developing inference tools for studying the tails of cross-sectional return distributions at high frequencies. We do this in Section 3.1 in the case when the intervals contain a systematic jump event and in Section 3.2 when this is not the case. Section 3.3 introduces a goodness-of-fit test for the power law of the cross-sectional return distribution tails.

3.1 Systematic Jump Tail Decay Index Estimation

We start with the case when the high-frequency intervals considered in the estimation contain systematic jumps. For those increments, the leading components of the tails of the asset returns are the systematic jumps. Idiosyncratic jumps in these intervals can be present but they are rare (the probability of an idiosyncratic jump in a stock over the interval is approximately proportional to the length of the interval) and hence do not distort the inference. As a result, we can develop inference tools by simply pretending that the other components of the asset prices are not present. We focus only on the positive systematic jump tails without lost of generality.

We can build an estimator using the power law tail approximation in (2.2). More specifically, using the discretized price processes, we propose the following estimator of ξ_S^+ :

$$\widehat{\xi}_S^+ = \frac{1}{\widehat{M}_N^{S+}} \sum_{i=1}^{N} \sum_{j \in \widehat{T}_n, \widehat{T}_n \neq \emptyset} \log\Big(\frac{\psi^+(\Delta_j^n p_i)}{\rho_N^S}\Big) \mathbf{1}_{\{\psi^+(\Delta_j^n p_i) > \rho_N^S\}}, \tag{3.1}$$

where

$$\widehat{M}_N^{S+} = \sum_{i=1}^{N} \sum_{j \in \widehat{T}_n, \widehat{T}_n \neq \emptyset} \mathbf{1}_{\{\psi^+(\Delta_j^n p_i) > \rho_N^S\}}, \tag{3.2}$$

and for some sequence $\rho_N^S \to \infty$. This is simply the Peak-Over-Threshold (POT) estimator. Theorem 1 provides the central limit theorem (CLT) for $\widehat{\xi}_S^+$. In its statement and henceforth we denote $\mathcal{C}$-conditional convergence in law with $\xrightarrow{\mathcal{L}|\mathcal{C}}$.

Theorem 1 *For the process $\{p_{it}\}_{i \geq 1}$ defined in (2.1), assume Assumptions 1–5 and*

Condition SJ hold. Then

$$\sqrt{\widehat{M}_N^{S+}}(\widehat{\xi}_S^+ - \xi_S^+) \xrightarrow{\mathcal{L}|\mathcal{C}} N\big(0, (\xi_S^+)^2\big), \tag{3.3}$$

where $N(0, \sigma^2)$ *denotes normal distribution with zero mean and variance* σ^2.

A feasible CLT follows immediately by replacing ξ_S^+ in the variance term by $\widehat{\xi}_S^+$. We note that the number of times of big systematic jumps over a given interval is fixed but since systematic jumps have a pervasive effect on the entire cross-section of assets, we can use most assets' returns in the inference. The rate of convergence of the estimator is determined by the number of asset returns used in the estimation. This, in turn, depends on how accurately does the power law describe the jump distribution in the tails. It depends also on the sampling frequency as this determines the size of the "residual" components of the asset prices. The condition restricting the number of observations used in the estimation is given in Condition SJ.

3.2 Idiosyncratic Jump Tail Decay Index Estimation

We turn next to the case when the high-frequency increments used in the estimation do not contain systematic jumps. When this is the case, the tail behavior of the cross-sectional return distribution is governed by the idiosyncratic jumps. From (2.3), the idiosyncratic jump tails can be approximated by the power law with tail decay parameters $\xi_I^{\pm}$. Therefore, we propose the following estimator of ξ_I^+:

$$\widehat{\xi}_I^+ = \frac{1}{\widehat{M}_N^{I+}} \sum_{i=1}^{N} \sum_{j \in \widehat{T}_n^c} \log\Big(\frac{\psi^+(\Delta_j^n p_i)}{\rho_N^I}\Big) \mathbf{1}_{\{\psi^+(\Delta_j^n p_i) > \rho_N^I\}}, \tag{3.4}$$

where

$$\widehat{M}_N^{I+} = \sum_{i=1}^{N} \sum_{j \in \widehat{T}_n^c} \mathbf{1}_{\{\psi^+(\Delta_j^n p_i) > \rho_N^I\}}, \tag{3.5}$$

and for some sequence $\rho_N^I \to \infty$. The CLT for $\widehat{\xi}_I^+$ is given in the next theorem.

Theorem 2 *For the process* $\{p_{it}\}_{i \geq 1}$ *defined in equation* (2.1)*, invoke Assumptions*

1, 2, 4, 5 and suppose Condition IJ holds. Then

$$\sqrt{\widehat{M}_N^{I+}}\,(\widehat{\xi}_I^+ - \xi_I^+) \xrightarrow{\mathcal{L}|\mathcal{C}} N\big(0, (\xi_I^+)^2\big). \tag{3.6}$$

A feasible CLT follows readily by replacing ξ_I^+ in the variance term by $\widehat{\xi}_I^+$. The above result appears similar to that for $\widehat{\xi}_S^+$. However, a key difference arises due to the fact that the number of stocks exhibiting idiosyncratic jumps over a single time interval is asymptotically small, as the sampling interval shrinks towards zero, because the probability of an idiosyncratic jump in a given stock is approximately proportional to the length of the short time interval. This is unlike the systematic jump scenario as, by definition, they materialize for a nontrivial number of assets simultaneously. Furthermore, the set of high-frequency increments not containing a systematic jump grows asymptotically, while the number of systematic jumps remains fixed. Thus, we can pool many more increments for estimation of the idiosyncratic tail distribution than we can for the systematic jump tails.

As for $\widehat{\xi}_I^+$, the rate of convergence of $\widehat{\xi}_I^+$ is governed by the number of increments employed for inference. This, in turn, hinges on the approximation error by the power law in the tails and the size of the discretization error, with the latter depending on the sampling frequency. This feature is captured by Condition IJ.

3.3 Goodness-of-Fit Test for Cross-Sectional Return Tails

We now develop a goodness-of-fit test for the tail power law. We rely on the Kolmogorov-Smirnov (KS) test statistic (see, e.g., Clauset et al. (2009)) for this purpose.

For the systematic jumps, our KS statistic is given by,

$$D_N^S \;=\; \sup_x \left| F_{N,t}^S(x) - P_{N,t}^S(x) \right|, \tag{3.7}$$

where $F_N^S(x)$ is the empirical tail distribution of the systematic jumps,

$$F_N^S(x) \;=\; \frac{1}{\widehat{M}_N^{S+}} \sum_{i=1}^{N} \sum_{j \in \widehat{T}_n, \widehat{T}_n \neq \emptyset} \mathbf{1}_{\{\psi^+(\Delta_j^n p_i) > x\}}, \quad \text{for } x \geq \rho_N^S, \tag{3.8}$$

and $P_N^S(x)$ is the tail probability implied by the estimated Pareto distribution,

$$P_N^S(x) \;=\; \left(\frac{x}{\rho_N^S}\right)^{-1/\widehat{\xi}_S^+}, \quad \text{for } x \geq \rho_N^S, \tag{3.9}$$

with $\widehat{\xi}_S^+$ defined in equation (3.1).

The next theorem characterizes the key property of our proposed KS statistic.

Theorem 3 *Suppose the assumptions of Theorem 1 apply with $\tau_S^+(x) \equiv 0$ for all $x \geq \rho_N^S$. Then,*

$$\sqrt{\widehat{M}_N^{S+}}\, D_{N,t}^S \;\xrightarrow{\mathcal{L}|\mathcal{C}}\; \mathcal{K}^{S+},$$

where $\mathcal{K}^{S+}$ is defined in Appendix E.

The limit distribution $\mathcal{K}^{S+}$ is that of a KS statistic based on a sample of the same size as the one of our estimator from an exact power-law tail distribution. We can estimate the quantiles of this distribution via simulation.

By replacing the subindex S with I and the set T_n with T_n^c, we also have the parallel results about the goodness-of-fit test for the power law characterization of the idiosyncratic jump tails. We give the theoretical results in Appendix F.

4 Monte Carlo Study

4.1 Setup

We use the following model in our simulation study:

$$\begin{aligned} p_{jt} \;&=\; \int^t \beta_j \sqrt{V_t}\, dW_t \;+\; \int^t \sqrt{V_s}\, d\widetilde{W}_{js} \;+\; \int^t \lambda_{is}\, dL_s \;+\; \int^t \int_{\mathbb{R}} x\, \mu_i(ds, dx), \\ dV_t \;&=\; 8.3\,(0.025 - V_t)\, dt \;+\; \sqrt{V_t}\,(-0.1\, dW_t + 0.2\,\sqrt{0.75})\, dB_t\,, \end{aligned}$$

where $\{\widetilde{W}_{js}\}_{j=1,\ldots,N}$, W_t, and B_t are independent standard Brownian motions. The factor exposures to diffusive systematic risk $\{\beta_j\}_{j=1,\ldots,N}$ are i.i.d. and drawn from $N(1, 0.5/3)$. The stochastic volatility (V_t) follows a square-root diffusion. The pa-

rameters of the volatility dynamics are set so that its annualized mean is 0.025 and the half life is one month (the unit of time is one year).

The calibration of the jumps is designed to mimic the tail behavior of stock jumps observed in our empirical application. Specifically, (L_t) is a simple point process with intensity $\nu_S = 1200\, V_t$ (and jumps of 1). This implies an average number of systematic jumps per day of approximately 0.12. For the systematic jump size, we draw λ_{is} from a Pareto distribution with $P(X < -x) = P(X > x) = 0.5(x/(0.1\sqrt{V_t}))^{-1/\xi_S}$. It follows that systematic jumps of size beyond 0.015 occur approximately 30 times per year. We set the tail decay index to $\xi_S \in \{0.4, 0.6\}$, representing the case of high/low systematic jump tail dispersion risk. The contribution of the systematic jumps to the quadratic variation of the stocks is about 10%–20%.

Finally, we generate the idiosyncratic jumps as follows. The jump compensators of μ_i are $\varphi_{it}^{\pm} = 30V_t$, and $\int_x^{\infty} \nu_{\phi}^{\pm}(s)ds = 1000(x/0.003)^{-1/\xi_I}$. The tail shape index is set to be $\xi_I \in \{0.4, 0.6\}$, corresponding to the cases with high/low tail dispersion risk. Under the above setting, positive/negative jumps account for 8% of the 10-minute returns, and the jump sizes are greater than 0.003. The contribution of the idiosyncratic jumps to the total return asset variation is about 30%–45%. These parameters are calibrated to mimic the tail behavior of idiosyncratic jumps observed in the real data. The combinations of ξ_S and ξ_I for different settings are collected in Table 1.

Table 1: Parameter settings for ξ_S and ξ_I in the Monte Carlo.

Model	M1	M2	M3	M4
ξ_S	0.6	0.6	0.4	0.4
ξ_I	0.6	0.4	0.4	0.6

4.2 Results

We simulate the asset prices for 1000 days/years when estimating idiosyncratic/systematic jump tail shape indices and sample at the 10-minute frequency. The number of stocks in the cross-section is $N = 250$ or 500. We identify the systematic jump times via the

procedure described in Appendix A. Next, we estimate the tail shape indices of the cross-sectional return distribution on the two disjoint sets including and excluding the systematic jump times. The idiosyncratic and systematic jump tail shape indices are estimated on a daily and yearly basis, respectively. The finite-sample performance of the resulting tail shape index estimators is summarized in Table 2 while that of the goodness-of-fit power law tail test is provided in Table 3.

Overall, the tail shape estimators perform well in various settings. Similarly, the empirical size of the goodness-of-fit test approximates the corresponding nominal level across different considered configurations fairly well. Not surprisingly, the estimation accuracy increases as the number of assets N grows. Moreover, the truncation level determining the number of increments used in the estimation impacts the estimation in a predictable way. Specifically, a higher truncation level generates noisier estimates while a lower truncation threshold leads to an increase in the bias due to the influence of the continuous return component.

5 Empirical Evidence for Cross-Sectional Tails

5.1 Data and Systematic Jump Detection

We focus on the S&P 500 Index constituent stocks over the period 2003–2022. The high-frequency price data are obtained from the TAQ database. We sample the prices each 10 minutes from 09:35 EST to 15:55 EST using the previous-tick approach and obtain 38 intraday 10-minute log returns. Following common data cleaning procedures (e.g., Aït-Sahalia et al. (2011)), "bounce back"s are removed. Finally, we use the SPY ETF for the S&P 500 Index as our market proxy. Holidays and half-trading days are excluded. In total, we have about 450 stocks each day and there are 4,993 full trading days in our sample.

We conduct our analysis on market-neutral asset returns, i.e., we use the returns of positions that are long an individual stock and short the market index. It is readily seen that, subject to mild local boundedness conditions on the market index, the theoretical results in Section 3 continue to apply when the estimator is based on market-neutral rather than raw returns. We adopt this approach because it facilitates

Table 2: Simulation results of the jump tail index estimation. The reported values are the median and interquarter range (IQR) from 1000 replications.

	Truncation Level					
	$\bar{\nu}_\phi(\rho_N) = 0.07$		$\bar{\nu}_\phi(\rho_N) = 0.05$		$\bar{\nu}_\phi(\rho_N) = 0.03$	
Model: True Value	**Median**	**IQR**	**Median**	**IQR**	**Median**	**IQR**
N=250						
$M1:\ \xi_S = 0.6$	0.607	[0.563 0.651]	0.609	[0.555 0.666]	0.623	[0.540 0.695]
$M1:\ \xi_I = 0.6$	0.582	[0.564 0.601]	0.577	[0.558 0.600]	0.563	[0.537 0.592]
$M2:\ \xi_S = 0.6$	0.572	[0.524 0.618]	0.559	[0.512 0.619]	0.547	[0.473 0.619]
$M2:\ \xi_I = 0.4$	0.440	[0.427 0.453]	0.415	[0.402 0.429]	0.380	[0.365 0.398]
$M3:\ \xi_S = 0.4$	0.375	[0.361 0.388]	0.368	[0.353 0.383]	0.354	[0.338 0.376]
$M3:\ \xi_I = 0.4$	0.439	[0.427 0.451]	0.414	[0.401 0.426]	0.379	[0.365 0.395]
$M4:\ \xi_S = 0.4$	0.393	[0.378 0.412]	0.394	[0.373 0.416]	0.392	[0.364 0.425]
$M4:\ \xi_I = 0.6$	0.580	[0.564 0.597]	0.575	[0.557 0.595]	0.561	[0.536 0.586]
N=500						
$M1:\ \xi_S = 0.6$	0.567	[0.496 0.649]	0.565	[0.488 0.666]	0.566	[0.466 0.687]
$M1:\ \xi_I = 0.6$	0.582	[0.570 0.597]	0.577	[0.564 0.597]	0.565	[0.546 0.587]
$M2:\ \xi_S = 0.6$	0.549	[0.461 0.624]	0.541	[0.433 0.630]	0.518	[0.388 0.633]
$M2:\ \xi_I = 0.4$	0.441	[0.431 0.451]	0.416	[0.406 0.428]	0.382	[0.370 0.395]
$M3:\ \xi_S = 0.4$	0.378	[0.367 0.389]	0.373	[0.361 0.387]	0.361	[0.345 0.376]
$M3:\ \xi_I = 0.4$	0.439	[0.430 0.449]	0.414	[0.405 0.426]	0.381	[0.370 0.393]
$M4:\ \xi_S = 0.4$	0.384	[0.372 0.395]	0.378	[0.364 0.391]	0.366	[0.348 0.385]
$M4:\ \xi_I = 0.6$	0.581	[0.569 0.594]	0.576	[0.562 0.591]	0.562	[0.545 0.582]

Table 3: Simulation results of the goodness-of-fit test. The reported values are the empirical size from 1000 replications.

	Truncation Level					
	$\bar{\nu}_\phi(\rho_N) = 0.07$		$\bar{\nu}_\phi(\rho_N) = 0.05$		$\bar{\nu}_\phi(\rho_N) = 0.03$	
Significance Level	0.05	0.01	0.05	0.01	0.05	0.01
N=250						
$M1:\ \xi_S = 0.6$	0.081	0.023	0.079	0.008	0.016	0.004
$M1:\ \xi_I = 0.6$	0.089	0.023	0.048	0.009	0.035	0.008
$M2:\ \xi_S = 0.6$	0.032	0.007	0.023	0.002	0.005	0.000
$M2:\ \xi_I = 0.4$	0.083	0.032	0.040	0.009	0.039	0.009
$M3:\ \xi_S = 0.4$	0.071	0.017	0.061	0.010	0.052	0.004
$M3:\ \xi_I = 0.4$	0.069	0.034	0.037	0.009	0.039	0.009
$M4:\ \xi_S = 0.4$	0.192	0.058	0.231	0.095	0.251	0.108
$M4:\ \xi_I = 0.6$	0.081	0.020	0.042	0.008	0.032	0.008
N=500						
$M1:\ \xi_S = 0.6$	0.039	0.011	0.025	0.005	0.004	0.000
$M1:\ \xi_I = 0.6$	0.102	0.035	0.04	0.007	0.025	0.005
$M2:\ \xi_S = 0.6$	0.029	0.002	0.017	0.002	0.004	0.000
$M2:\ \xi_I = 0.4$	0.134	0.077	0.04	0.017	0.021	0.006
$M3:\ \xi_S = 0.4$	0.092	0.019	0.093	0.024	0.089	0.013
$M3:\ \xi_I = 0.4$	0.086	0.049	0.037	0.016	0.024	0.006
$M4:\ \xi_S = 0.4$	0.098	0.025	0.127	0.033	0.115	0.048
$M4:\ \xi_I = 0.6$	0.078	0.022	0.043	0.008	0.027	0.007

identification of the non-market systematic jump risk, see Jacod et al. (2024).

We start with detection of the systematic jump times, i.e., determining the set $\widehat{T}_n$. The systematic jumps can be split into those that trigger jumps in the market index and those that do not. For the former, we use the high-frequency observations on the SPY index and a standard truncation procedure. For the non-market systematic jumps, we use the method proposed by Jacod et al. (2024), see equations (15)–(17) in that paper. Further details on the systematic jump detection are provided in Appendix A. Upon applying these jump detection procedures, we find that 7% of the days in our sample contain market jumps and 9% involve non-market systematic jumps. In total, the daily systematic jump rate (market and non-market) is 12%. That is, there is one systematic jump about every 8 trading days.

5.2 The Tails of the Cross-Sectional Return Distributions

5.2.1 In the Presence of Systematic Jumps

We first focus on the high-frequency intervals containing systematic jumps. In order to obtain a reasonable large sample size, we aggregate the systematic jumps for a year. For illustration, we pick two years, 2008 and 2016, representing a case with a high and a case with a moderate level of volatility. We display the distribution of the 10-minute S&P 500 stock market-neutral returns when there are systematic jumps during each of these two years in Figure 1. For ease of comparison, we standardize the returns to have a unit standard deviation within each cross-section. The plot reveals that the cross-sectional distributions of the systematic jumps in both years are heavy-tailed. We also note that the year 2016 features a somewhat higher number of detected systematic jumps than 2008.

We next fit a power law to the right and left return tails, respectively, using the procedures developed in Section 3. We first transform the log returns to arithmetic returns using $\psi(x) = \exp(|x|) - 1$. We then use all the 10-minute return intervals within the year that contain a systematic jump to estimate the Pareto distribution

$$P(X > x | X > x_m) = \left(\frac{x}{x_m}\right)^{-1/\xi_t}, \text{ for } x \geq x_m,$$

where x_m equals the $(1-\tau)$-return quantile. We use the threshold level $\tau = 0.05$. In Figure 2, we plot the logarithm of the empirical tail probabilities along with the fitted values implied by the estimated Pareto distributions. We observe that the cross-sectional return tails appear well approximated by power laws. Our estimates for ξ_t in 2016 are 0.43 for the left and 0.48 for the right tail. Those for 2008 are 0.65 for the left and 0.64 for the right tail. These estimates imply near symmetric tails in both years. We also note that the tails are somewhat fatter in 2008 than in 2016.

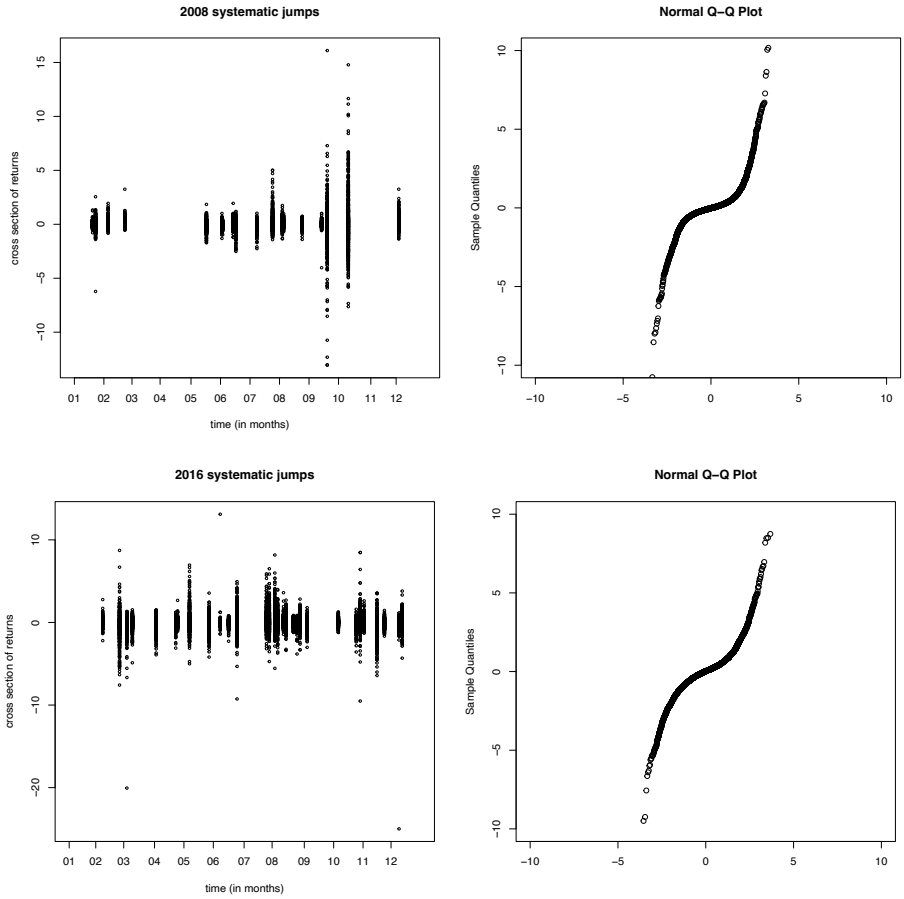

Figure 1: Distribution of S&P 500 Index stocks' 10-minute market-neutral returns when there are systematic jumps for the year 2008 and year 2016. The returns are normalized to have a standard deviation of one.

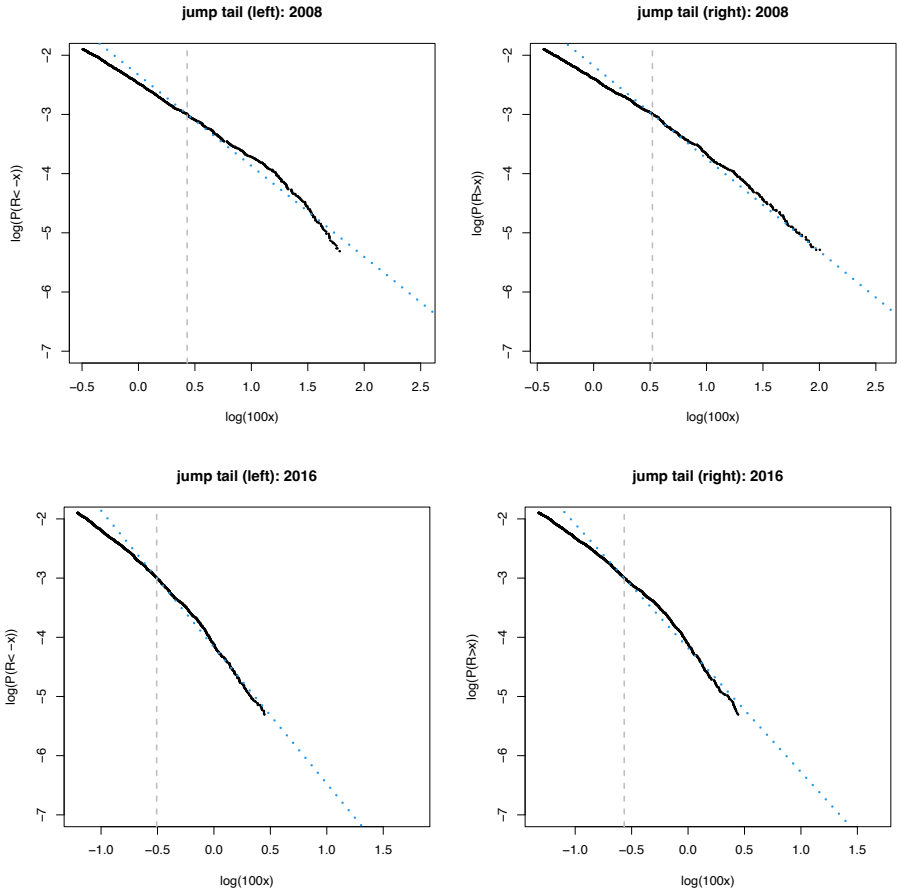

Figure 2: Empirical tail distribution and the fitted Pareto tail of S&P 500 Index stocks' 10-minute returns when there are systematic jumps during the year 2008 and the year 2016.

5.2.2 Absent Systematic Jumps

We now continue with the increments that do not contain systematic jumps. Since these constitute the vast majority of the increments in the sample, we can perform this analysis at the daily level. We pick two representative days for illustration, October-10-2008 and March-4-2016, from the two years used above for analysis of the systematic jumps. On October 10, 2008, the market features elevated volatility while on March 4, 2016, market volatility is about average. We plot the distribution of the 10-minute S&P 500 stock market-neutral returns on these two days in Fig-

ure 3. There are no detected systematic jumps on either of the two days. Once more, we standardize the returns to have a cross-sectional unit standard deviation. The plot corroborates the hypothesis of fat-tailed cross-sectional return distributions. Although the levels of volatility on the two days are very different, the heavy-tailedness of the two cross-sectional return distributions appear similar.

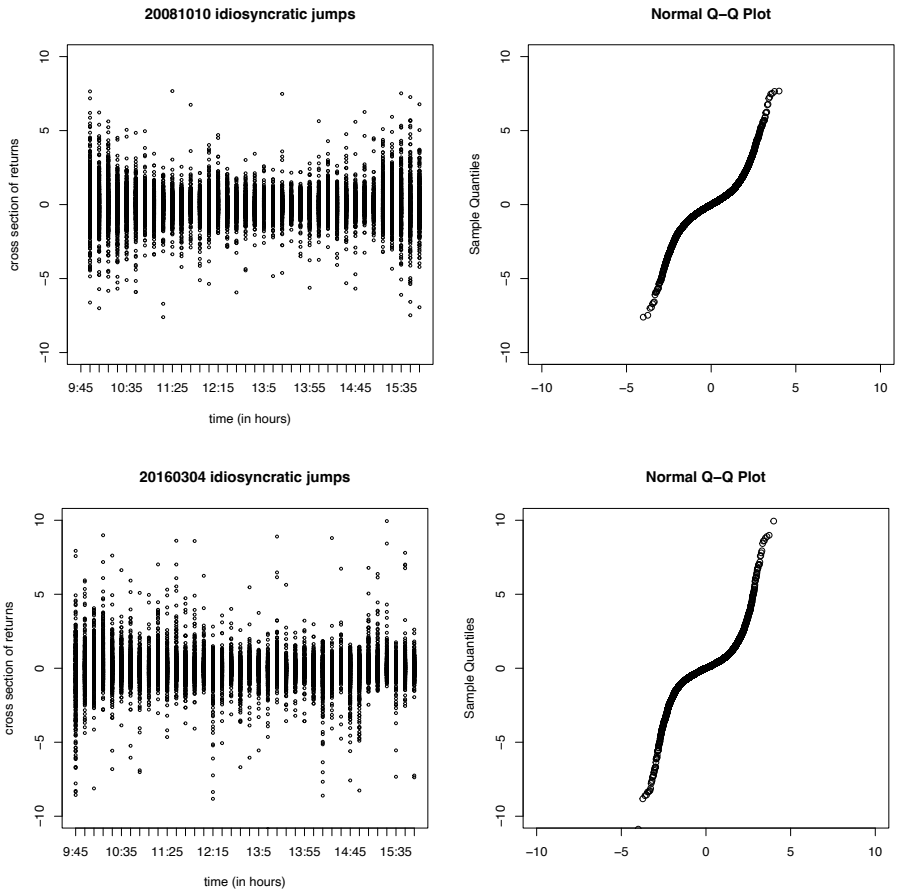

Figure 3: Distribution of S&P 500 stock 10-minute market-neutral returns on two representative days, 20081010 and 20160304. Systematic jumps are not detected on either of the two days. The returns are standardized to have a standard deviation of one.

Next, we go on to fit power laws to the tails of the cross-sectional return distributions using the approach developed in Section 3.2. In Figure 4, we plot the logarithm of the empirical tail probabilities, together with the fitted values by the estimated

Pareto distributions. Similar to the case of systematic jumps, we see that the power law provides a good fit for the tails of the cross-sectional return distributions in the absence of systematic jumps. The slope of the Pareto tail is given by $-\alpha_t = -1/\xi_t$. A flatter fitted tail probability line thus indicates a fatter tail distribution. Our estimates of the tail shape index, ξ_t, on March-4-2016 are 0.524 for left tail and 0.495 for right tail. Those for October-10-2008 are 0.415 and 0.440 for the left and right tails, respectively. This implies that the tails of the cross-sectional return distribution on March-4-2016 are slightly fatter than those on October-10-2008 despite the fact the volatility on October-10-2008 was much higher.

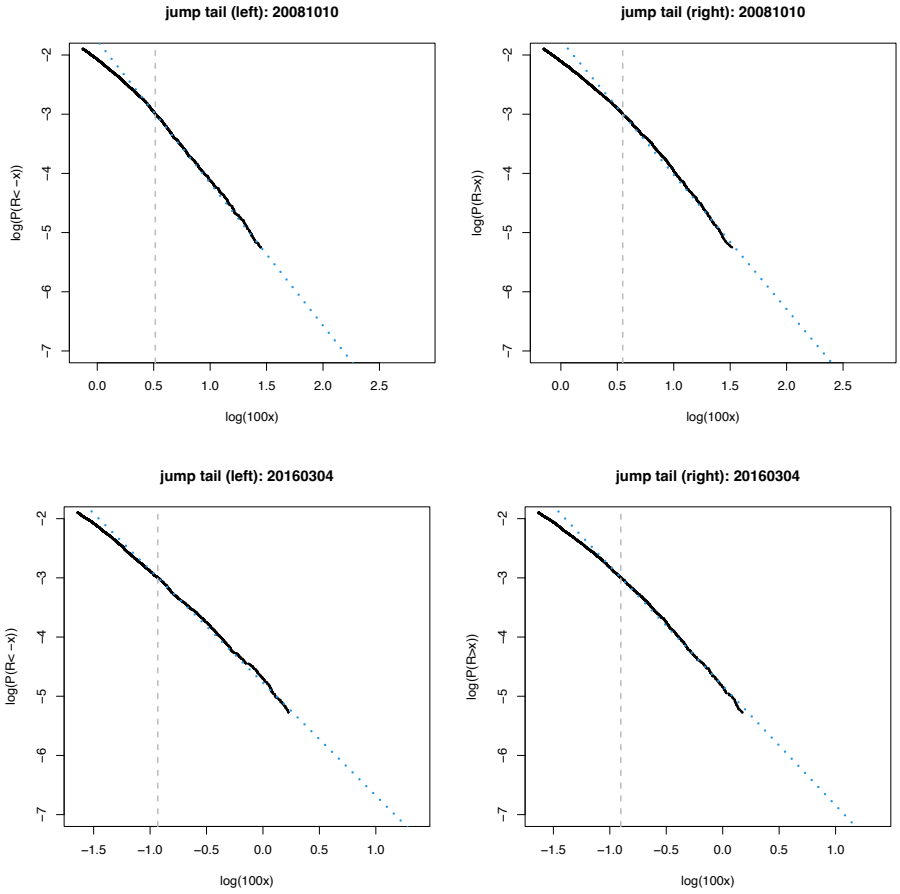

Figure 4: Empirical tail distribution and the fitted Pareto tail of S&P 500 Index stocks' 10-minute returns of the date 2008-10-10 and the date 2016-03-04. Systematic jumps are not detected on either of the two days.

Table 4: Goodness-of-fit test results for the power law of the jump tails. We report the proportions of rejections between 2003 and 2022. We test the power-law for the systematic jump tails using data in a moving one-year window and the idiosyncratic jump tail based on daily samples. The significant level is set to 5% and 1%.

Significant level	Power Law Tail Rejection Rate			
	Systematic jump		Idiosyncratic jump	
Goodness-of-Fit Test Rejection Rate				
	left tail	right tail	left tail	right tail
significance level= 5%				
$\bar{\nu}_\phi(\rho_N) = 0.07$	0.039	0.123	0.171	0.164
$\bar{\nu}_\phi(\rho_N) = 0.05$	0.039	0.075	0.114	0.099
$\bar{\nu}_\phi(\rho_N) = 0.03$	0.013	0.052	0.073	0.064
significance level= 1%				
$\bar{\nu}_\phi(\rho_N) = 0.07$	0.013	0.044	0.056	0.053
$\bar{\nu}_\phi(\rho_N) = 0.05$	0.004	0.018	0.027	0.027
$\bar{\nu}_\phi(\rho_N) = 0.03$	0.000	0.000	0.016	0.014

5.3 Goodness-of-Fit Test for Tails

We now test formally whether the tails of the cross-sectional return distributions are approximated well by the Pareto distribution. We perform the goodness-of-fit test for the tails of returns with and without systematic jumps separately. We use three different cutoffs for the tails corresponding to 7%, 5%, and 3% return quantiles. The test for the systematic jumps is based on a 252-day moving window, while the test for the idiosyncratic jumps is performed on a daily basis. Table 4 summarizes the percentage of days when the power law distribution is rejected over our sample. Overall, the reported results show that the tails of the cross-sectional return distribution are well described by a power law. Indeed, the rejection rates of the test are low and roughly match the nominal significance levels of the test.

5.4 Time Series of Cross-Sectional Tail Shape Indices

This section explores the time-series variation in the cross-sectional tail shape index. The systematic jump tail shape index is estimated every day based on the 10-minute returns for the past 252 days when systematic jumps occur.[2] The idiosyncratic jump tail shape index is estimated on a daily basis.

The time series of the cross-sectional tail shape indices are depicted in Figure 5. For comparison, we plot the market volatilities and the common idiosyncratic volatilities in the bottom panel of the figure. The daily market volatility estimate is the square-root of the daily realized variance of the SPY index. The daily common idiosyncratic volatility estimate is the square-root of the cross-sectional average of daily idiosyncratic realized variances. The latter are defined as the realized variances of the assets' returns minus their market beta estimates times the market return. To better assess the low-frequency pattern in the various series, Figure 6 provides 6-month (132-day) moving averages of the series plotted in Figure 5.

We can draw several conclusions from these two plots. First, there is considerable variation in the tail shape of the cross-sectional return distributions over time. The range of the shape indices is between 0.3 and 0.6 for systematic jumps and between 0.35 and 0.5 for idiosyncratic jumps. The associated shape parameter $\alpha = 1/\xi$ is about 2–3.5, which is comparable to the shape parameter estimated in typical financial time series. Second, the left and right tail shapes appear similar. This is easier to see for the returns that do not contain systematic jumps. For the ones that contain jumps, there are some differences in the left and right tail estimates but some of these differences are likely due to noise.[3] Third, there appears to be little relation between the variation of the tail shapes of returns with and without systematic jumps. For example, the cross-sectional return distribution appears fat-tailed during the crisis of 2008, regardless of whether the returns included systematic jumps or not. However, the opposite conclusion applies after the onset of the pandemic-related market turbulence in 2020. Finally, the dynamics of the tail shapes of the cross-sectional return

[2]We have also checked the index estimated using moving window of 22 days. The results are noisier and hence less informative due to the small sample size.

[3]We also check the systematic jumps separately based on SPY jumps, and the latent systematic jumps. For both type of systematic jumps, the right and left tails appear similar, while there is slightly larger variation in SPY jumps, but these difference may be also likely due to noise.

Figure 5: Above: Time series of estimated systematic jump tail shape index using the data in the past 252 days. Middle: Daily idiosyncratic jump tail shape index. Below: Daily market volatilities and common idiosyncratic volatilities.

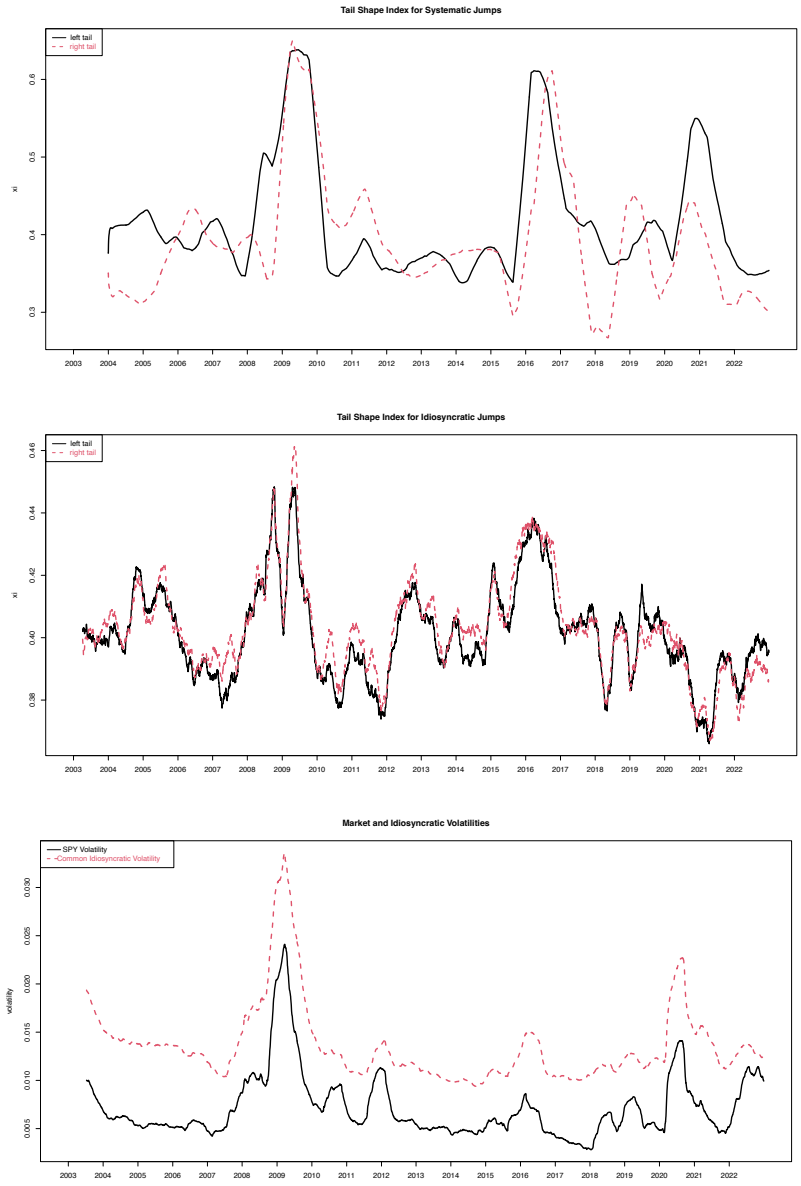

Figure 6: Time series of 132-day moving averages of the estimated systematic jump tail shape index (above), daily idiosyncratic jump tail shape index (middle), and the daily market volatilities and common idiosyncratic volatilities (below).

distribution seems distinct from that of market and common idiosyncratic volatility.

6 Asset Pricing Implications

Given the significant and distinct time-series variation in the tail shape of the cross-sectional return distribution, we now ask whether it is a source of priced risk. We explore this using the entire pool of stocks traded on NYSE/AMEX/NASDAQ between 2003 and 2022. The daily stock return data is obtained from CRSP, excluding only micro-cap stocks with size below the 20% quantile of the NYSE breakpoints and stocks with a share price under \$5.

6.1 Pricing of Shocks to the Systematic Jump Tails

We start by assessing whether shocks to ξ_S are priced. Because the empirical evidence in the previous section revealed no substantive differences between the left and right tails, we combine the two estimates to improve the efficiency of the inference. That is, we use $\bar{\xi}_{S;t} = 2/(\alpha^L_{S;t} + \alpha^R_{S;t})$, where $\alpha^L_{S;t} = 1/\xi^-_{S;t}$, and $\alpha^R_{S;t} = 1/\xi^+_{S;t}$. We then compute the change between adjacent non-overlapping periods of h days,

$$\Delta\xi_{S;t,h} \;=\; \frac{1}{h}\sum_{j=t-h+1}^{t}\bar{\xi}_{S;j} \;-\; \frac{1}{h}\sum_{j=t-2h+1}^{t-h}\bar{\xi}_{S;j}. \tag{6.1}$$

We focus on monthly tail dispersion risk innovations and correspondingly set $h = 22$ (with the unit of time now being one trading day) in the analysis henceforth. Given our definitions, a positive (negative) tail shape shock represents an increase (decrease) in the fat-tailedness of the cross-sectional return distribution during times of systematic jumps. We estimate the exposure of the returns to such systematic jump tail shocks using the following standard time-series regression with $h = 22$,

$$R_{i,t,h} \;=\; a_i + b_i\,\Delta\xi_{S;t,h} + \varepsilon_{i,t}\,, \tag{6.2}$$

where $R_{i,t,h}$ is the h-day cumulative returns from day $t-h+1$ to t.

For each day t, we run the regression in equation (6.2) using the data from the

past 1260 days and get the estimated loadings $(\hat{b}_i)_{i\geq 1}$. We then sort the stocks into 5 groups based on $(\hat{b}_i)_{i\geq 1}$. We form equal- and value-weighted portfolios for each quintile group and track the out-of-sample portfolio returns. Beyond an out-of-sample holding window of one month ($H = 22$), we also explored $H = 66$. We summarize the portfolio performance in Table 5 for the one-month holding window. Results for the three-month holding window are qualitatively similar and deferred to Appendix B.

Panel A of Table 5 reports the out-of-sample annualized average returns for the 5 quintile portfolios and the low-minus-high portfolio (LmH_{SysJ}) that goes long/short the quintile portfolio with the lowest/highest exposure to systematic jump tail dispersion risk shocks. We also report the t-statistics of the returns based on Newey-West standard errors using 22 lags. We observe a monotonic decline in the average returns from the high beta portfolio to the low beta portfolio, based on both equal- and value-weighting schemes. The high (low) beta portfolio has an average positive (negative) exposures to the systematic jump shocks. The equal-weighted LmH_{SysJ} portfolio has an annualized return of 5.13% with a t-statistic of 2.67, that is, equivalent to an annualized Sharpe ratio (SR) of 0.62, while the value-weighted LmH_{SysJ} portfolio has an annualized return of 5.23% with a t-statistic of 2.11, or a SR of 0.49.

We further evaluate the significance of the LmH_{SysJ} portfolio's returns after controlling for a variety of systematic risk factors used in previous research. We consider the following factors: the Market, Fama-French three/five/six factors (FF3/FF5/FF6, Fama and French (1993, 2015, 2018)). In addition, we include the tail risk factor by Kelly and Jiang (2014), the idiosyncratic risk factor (idiorisk) of Ang et al. (2006))[4], and the CiV factor of Herskovic et al. (2016).[5] Furthermore, we include the HmL portfolio sorted using idiosyncratic jump tail shape shock betas, introduced in Section 6.2 below, as a control factor. The results are summarized in Panel B of Table 5. We see that the LmH_{SysJ} portfolio has a significant alpha controlling for most of the factors. For example, under FF6, the alpha of the equal-weighted LmH_{SysJ} portfolio is 5.11% ($t = 2.66$), the alpha of the value-weighted LmH_{SysJ} portfolio is 5.82% ($t = 2.29$). After controlling for the tail-risk factor of Kelly and Jiang (2014), the

[4]Replicated tail-risk beta LS sorted portfolio of Kelly and Jiang (2014) and the idiosyncratic risk factor portfolio are obtained from Chen and Zimmermann (2021).

[5]The CiV-beta LS portfolio monthly returns are obtained from https://bernardherskovic.com/data/

Table 5: Returns of systematic jump tail shock beta-sorted portfolios. The table reports out-of-sample annualized average returns (in percentage) and t-statistics for portfolios sorted on the cross-sectional jump tail beta. We sort stocks daily into quintile portfolios using jump tail betas that are estimated using daily returns over the past five years. The holding window of the portfolio is one month. We use all stocks traded on NYSE/AMEX/NASDAQ exchange with price above $5 and stock capitalization beyond the 20% NYSE size breakpoint. We consider both equal- and value-weighted portfolios. The out-of-sample period is between the years 2004 and 2022. Panel A reports the portfolios' average betas to the jump tail shocks and annualized returns, all in percentage, and Panel B reports the alphas under CAPM, FF3/FF5/FF6 models, while controlling for the tail-risk factor (Kelly and Jiang (2014)), the CiV factor (Herskovic et al. (2016)), the idiosyncratic risk factor (Ang et al. (2006)), and the HmL_{IdioJ} portfolio sorted using idiosyncratic jump shock exposures. The t-statistics are computed based on Newey-West (Newey and West (1987)) standard errors with lag length equal to the holding window.

		Equal-weight		**Value-weight**	
		Panel A: Mean Portfolio Returns			
Portfolio	**Beta Ret**	**t-stat**	**Ret**	**t-stat**	
H	1.77	10.74	2.59	10.91	3.02
Q4	-0.05	13.00	3.47	10.23	3.34
Q3	-0.93	13.66	3.59	13.50	4.58
Q2	-1.83	14.44	3.71	15.82	5.10
L	-3.81	15.87	3.53	16.14	4.24
LmH_{SysJ}		5.13	2.67	5.23	2.11
		Panel B: Abnormal Return of LmH_{SysJ} Portfolio			
Measure		**Ret**	**t-stat**	**Ret**	**t-stat**
CAPM alpha		3.66	1.92	3.91	1.55
FF3 alpha		3.90	2.08	4.35	1.74
FF5 alpha		4.46	2.31	5.13	2.00
FF6 alpha		5.11	2.66	5.82	2.29
CAPM+tailrisk alpha		4.07	2.02	4.82	1.86
FF6+tailrisk alpha		5.02	2.54	5.92	2.28
CAPM+CiV alpha		4.32	1.83	5.90	1.79
FF6+CiV alpha		5.25	2.19	6.59	1.98
CAPM+idiorisk alpha		4.84	2.19	5.57	2.02
FF6+idiorisk alpha		5.02	2.54	6.23	2.42
CAPM+HmL_{IdioJ} alpha		4.02	2.13	4.98	1.93
FF6+HmL_{IdioJ} alpha		5.43	2.89	6.94	2.64

CiV factor of Herskovic et al. (2016), the idiosyncratic risk factor of Ang et al. (2006), and the effect of idiosyncratic jump tail risks (HmL_{IdioJ}), to be introduced below, the alphas of our LmH_{SysJ} portfolio remain significant.

We next compute the pairwise correlation between the tail dispersion risk innovations used for our portfolio sorting and the control factors explored in Panel B of Table 5. We summarize the results in Table 6. It shows that the systematic jump tail-shape shocks have little correlation with the common systematic risk factors, corroborating the hypothesis that systematic jump tail shape shocks represent risks not captured by prior advocated asset pricing factors.

Table 6: Correlations between the innovation in jump tail dispersion risks and the return factors. Reported values are pairwise correlation between the innovations of systematic jump risks, $Inno\xi_S$, idiosyncratic jump risks $Inno\xi_S$, obtained from equation (6.1), and return factors that include the Market (Mkt), FF factors (FF.SMB, FF.HML, FF.RMW, FF.CMA, FF.MOM), the tail-risk factor (Kelly and Jiang (2014)) denoted by tailrisk, the CiV factor (Herskovic et al. (2016)) denoted by CIV.LS, and the idiosyncratic risk factor (Ang et al. (2006)) denoted by idiorisk. In addition, we include the signals used to construct the CiV factor, that is the common idiosyncratic shocks (CiV. shock). The evaluation period is between 2004 and 2022.

	$Inno\xi_S$	$Inno\xi_I$
Mkt	0.003	-0.084
FF.SMB	-0.003	-0.006
FF.HML	0.007	0.011
FF.RMW	-0.005	-0.011
FF.CMA	0.030	-0.009
FF.MOM	0.004	-0.026
tailrisk	-0.030	0.007
CIV.LS	0.086	-0.022
CIV.shock	0.042	0.134
idiorisk	0.007	-0.011
$Inno\xi_S$	–	0.008

Finally, as a robustness check, in Appendix C, we report portfolio sorting results using different truncation levels in the systematic jump detection procedure. The

findings are qualitatively similar to those reported here.

Overall, our finding of a negative price response to positive ξ_S shocks implies that investors view periods, in which systematic jumps generate more extreme returns, as unfavorable states of the world. Stocks that do well during such times serve as hedges and require a lower risk premium. This is intuitive from a standard portfolio perspective, as systematic jumps constitute a major source of risk for strategies exposed to systematic risk factors. Enhanced and time-varying return dispersion induced by systematic jumps exacerbates the possibility of poor portfolio performance and renders efficient diversification more difficult. Increasing dispersion risk during times of large systematic return jump events is therefore disliked by investors. We further note that this phenomenon is similar to the beta risk documented in Boloorforoosh et al. (2020) who find that low market-betas tend to increase along with market risk and hence require an additional risk premium. The finding about the relation between beta dynamics and volatility is broadly consistent with the well documented observations that the returns will become more synchronized during volatile period (Solnik et al. (1996); Andersen et al. (2001).

6.2 Pricing of Shocks to the Idiosyncratic Jump Tails

We next study whether shocks to the tail shape parameter of idiosyncratic jump risk requires compensation. Note that, just like the strength of average idiosyncratic volatility, shocks to the tail shape parameter of the idiosyncratic jump risk is a form of aggregate risk. As for the systematic jump tails, we measure the idiosyncratic jump tail shape shocks using the innovations in the jump tail index $\xi_{I;t}$. Specifically, we use $\bar{\xi}_{I;t} = 2/(\alpha^L_{I;t} + \alpha^R_{I;t})$, where $\alpha^L_{I;t} = 1/\xi^-_{I;t}$, and $\alpha^R_{I;t} = 1/\xi^+_{I;t}$ represent the parameters estimated from the left and right idiosyncratic jump tails, respectively. We have performed the same analysis using separate left and right tail shape indices, generating similar results to those based on the average of the two reported here.

Following the portfolio formation approach of Section 6.1, we sort stocks on the basis of their exposures to $\bar{\xi}_{I;t}$. We summarize the results in Table 7. The out-of-sample evaluation period is between 2004 and 2022, and the holding-window for the portfolio is one month. Table 7 reveals that, unlike the portfolios sorted on

exposure to systematic jump tail shape risk, there is a decreasing pattern in the average returns from the high to the low beta portfolio, both for equal-weighting and value-weighting schemes. The high (low) beta portfolio has positive (negative) exposures to the idiosyncratic jump shocks. The equal-weighted HmL_{IdioJ} portfolio, that is, the portfolio that goes long/short the quintile portfolio with the highest/lowest exposure to idiosyncratic tail shape shocks, has annualized returns of 3.19% with a t-statistic of 1.98 (annualized SR of 0.46). The returns for the value-weighted portfolio is 3.98% with a t-statistic of 1.92 (annualized SR of 0.45). Furthermore, the HmL_{IdioJ} portfolio's alphas are significant after controlling for a variety of common systematic risk factors. Sorting results for a three-month holding period are similar to those for one month and are provided in the Appendix B.

Consistent with the significance of the alphas of the HmL_{IdioJ} portfolios, the shocks to the idiosyncratic jump tail shape index appear weakly and insignificantly correlated with the common systematic risk factors, as seen from Table 6.

We check the robustness of the portfolio sorting results for systematic jump detection for alternative thresholds in Appendix C. We find the results for idiosyncratic jump sorted portfolios consistent across the different tuning parameter settings.

Overall, our results suggest that positive shocks to ξ_I (a fattening of the idiosyncratic jump tail) are viewed favorably by investors, i.e., times featuring thicker idiosyncratic jump tails are good states of the world. Therefore, stocks that do well when ξ_I is high and positive earn a positive premium. How do we rationalize this pricing result which is the exact opposite to our finding from portfolio sorts based on ξ_S? We first reiterate that, although ξ_I is linked to idiosyncratic jumps, shocks to ξ_I still represent aggregate risk, as they impact the extent to which the cross-section experiences more or less extreme idiosyncratic jumps. However, this fact does not help us rationalize the sign of the pricing from a risk-based perspective. Instead, we note that these results are consistent with lottery-type preferences which imply that investors like stocks that can generate huge positive returns (winning the lottery). The lottery-like preferences has been evidenced in both equity and option market contexts, as documented in studies such as Boyer and Vorkink (2014); Blau et al. (2016) and Filippou et al. (2018). For such investors, episodes in which idiosyncratic jump tails grow fatter provide better upside potential and hence are preferred by

Table 7: Returns of idiosyncratic jump tail shock beta-sorted portfolios. The table reports out-of-sample annualized average returns (in percentage) and t-statistics for portfolios sorted based on cross-sectional jump tail beta. We sort stocks each day into quintile portfolios using jump tail betas. The jump tail betas are estimated using daily returns of the past five years. The holding window of the portfolio is one month. We use all stocks traded on NYSE/AMEX/NASDAQ exchange with price above $5 and stock capitalization beyond the 20% NYSE size breakpoint. Stocks are formed into equal- and value-weighted portfolios. The out-of-sample period is between 2004 and 2022. Panel A reports the portfolios' average betas to the idiosyncratic jump tail shocks and annualized returns, all in percentages, and Panel B reports the alphas under CAPM, FF3/FF5/FF6 models, controlling for the tail-risk factor (Kelly and Jiang (2014)), the CiV factor (Herskovic et al. (2016)), the idiosyncratic risk factor (Ang et al. (2006)), and the low-minus-high portfolio sorted using systematic jump tail exposures (LmH_{SysJ}). The t-statistics are based on Newey-West (Newey and West (1987)) standard errors using a lag length equals to the holding window.

		Equal-weight		**Value-weight**	
		Panel A: Average Portfolio Returns			
Portfolio	**Beta**	**Ret**	**t-stat**	**Ret**	**t-stat**
H	6.19	15.31	3.73	15.43	4.61
Q4	2.73	13.98	3.70	13.30	4.57
Q3	0.76	13.47	3.55	10.69	3.72
Q2	-1.19	13.19	3.41	11.11	3.66
L	-5.26	12.12	2.73	11.46	3.14
HmL_{IdioJ}		3.19	1.98	3.98	1.92
		Panel B: Abnormal Return of HmL_{IdioJ} Portfolio			
Measure		**Ret**	**t-stat**	**Ret**	**t-stat**
CAPM alpha		4.17	2.26	4.90	1.98
FF3 alpha		4.06	2.17	4.37	1.72
FF5 alpha		4.10	2.20	4.86	1.87
FF6 alpha		5.11	2.66	4.72	1.82
CAPM+tailrisk alpha		4.45	2.37	5.91	2.31
FF6+tailrisk alpha		4.44	2.37	5.92	2.28
CAPM+CiV alpha		3.82	1.86	5.52	2.33
FF6+CiV alpha		4.11	2.02	5.76	2.35
CAPM+idiorisk alpha		3.94	2.20	5.09	2.01
FF6+idiorisk alpha		4.22	2.32	5.65	2.16
CAPM+LmH_{SysJ} alpha		4.46	2.58	5.25	2.23
FF6+LmH_{SysJ} alpha		4.42	2.63	4.99	2.07

them.

6.3 Portfolio Combination

The results in Sections 6.1 and 6.2 demonstrate that the LmH_{SysJ} and HmL_{IdioJ} portfolios sorted based on the exposure to systematic and idiosyncratic jump tail shape shocks earn positive expected returns in the future. In addition, Table 6 shows that shocks to ξ_S and ξ_I appear nearly uncorrelated. Hence, not surprisingly, the HmL_{IdioJ} and LmH_{SysJ} portfolio returns are weakly related, with sample correlation coefficients equalling -0.11 and -0.07 for the equal- and value-weighted portfolios. Consequently, combining them should improve performance, as it does for Asness et al. (2013), who document substantial gains (in terms of Sharpe ratios) from combining value and momentum portfolios. Towards this end, we evaluate a simple equal-weighted combination of the HmL_{IdioJ} and LmH_{SysJ} portfolios. Denoting the return of the HmL_{IdioJ} (LmH_{SysJ}) portfolio of idiosyncratic (systematic) jump tail exposure by r_t^{IdioJ} (r_t^{SysJ}), the return of the combined portfolio (Comb) is given by,

$$r_t^{Comb} \;=\; 0.5\, r_t^{IdioJ} + 0.5\, r_t^{SysJ}.$$

We report the performance of this combined portfolio in Table 8.

Table 8: Return performance of the combined portfolio. The table reports average returns and abnormal returns under alternative linear factor models over our 2004-2022 sample. The portfolio holding period is one month. We also report t-statistics based on Newey-West (Newey and West (1987)) standard errors using a lag length equals to the holding period.

	Equal-weight		**Value-weight**	
Measure	**Ret**	**t-stat**	**Ret**	**t-stat**
MEAN	3.57	3.58	3.91	2.97
CAPM alpha	3.04	2.88	3.47	2.43
FF3 alpha	3.16	3.05	3.67	2.56
FF5 alpha	3.37	3.12	4.15	2.81
FF6 alpha	3.67	3.43	4.50	3.09
CAPM+tailrisk alpha	3.22	2.93	4.15	2.80
FF6+tailrisk alpha	3.64	3.30	4.72	3.12
CAPM+CiV alpha	3.82	1.86	5.52	2.33
FF6+CiV alpha	4.12	2.02	5.76	2.35
CAPM+idiorisk alpha	3.63	3.11	4.50	2.96
FF6+idiorisk alpha	3.51	1.80	4.85	3.24

Table 8 confirms that the performance of the combined portfolio improves over the two portfolios individually in terms of generating a higher return significance (and hence Sharpe ratio). For example, the t-statistic of the mean return is 3.58 (annualized SR is 0.83) for the combined one-month holding period portfolio under the equal-weighted scheme and 2.97 (annualized SR is 0.70) for value-weighted scheme. These numbers are significantly higher than their counterparts for the HmL_{IdioJ} and LmH_{SysJ} portfolios considered in isolation.

6.4 The Pricing of Shocks to Cross-Sectional Volatility

Our analysis has focused exclusively on the tail index of the cross-sectional return distribution. It is natural to ask whether other measures of the cross-sectional return

dispersion would generate a similar pricing performance? The obvious benchmark is a measure of the overall cross-sectional return volatility. To investigate this issue, we follow the same approach adopted in Sections 6.1 and 6.2 for analysis of the risk pricing exercise for shocks to the tail shape index. That is, we perform the identical portfolio sorting procedure, but replace the tail index ξ with cross-sectional volatility, estimated as the cross-sectional average of all squared returns for a given time increment. Furthermore, like in Sections 6.1 and 6.2, we consider separately the case with and without systematic jumps. We denote these cross-sectional volatility measures by $CSVol^{SysJ}$, and $CSVol^{IdioJ}$ for the cross-sectional volatilities when systematic jumps are present or absent, respectively. Table 10 reports the performance of the portfolios sorted on betas to shocks in $CSVol^{SysJ}$, while Table 11 reports the performance of the portfolios sorted on betas to shocks in $CSVol^{IdioJ}$.

First, we note that the mean returns and alphas for both cross-sectional volatility shock beta-sorted LmH portfolios are economically weaker and less statistically significant than that of jump tail-risk sorted portfolios. Second, importantly, for the cross-sectional volatilities, both pricing effects are negative. That is, as the volatility shock beta increases, we observe a market drop in the mean returns of the beta sorted portfolios, regardless of whether systematic jump are included in the cross-sectional volatility measure or not. This is, of course, to be expected. The high beta stocks are good performers when the market is subject to shocks that elevate volatility, and they therefore serve as relatives hedge against volatility shocks, all else equal, lowering their required risk compensation in equilibrium. But how do we reconcile these findings with our results for the pricing of tail risk dispersion?

The key distinction is that the diffusive volatility now will have a strong impact on our cross-sectional $CSVol$ return variation measures while, in the absence of systematic jumps, the tail shape distribution is governed by the idiosyncratic jumps. At the same time, we expect the systematic diffusive volatility to generate qualitatively identical pricing effects to the systematic jump variation. Consequently, even for return increments without systematic jumps, the diffusive volatility will tend to offset the effect of the idiosyncratic jump variation. Thus, we should anticipate some cancellation of the two pricing effects, which evidently suffices to reverse the prior results for idiosyncratic jump risk, when sorting on betas for shocks to $CSVol^{IdioJ}$. In

other words, inspection of the tail distribution is critical to identify the cross-sectional pricing implications of idiosyncratic jump risk. Moreover, this identification can only be achieved using returns observed over short intraday intervals, as the distribution of lower-frequency returns will reflect a complex time-varying mixture of components stemming from diffusive volatility and both idiosyncratic and systematic jumps.

6.5 Pricing of Shocks to Tails in Daily Returns

The above analysis are based on return tail measures obtained from the high-frequency data. A natural question is whether these results are preserved at a lower frequency. To investigate this problem, we use daily data to replicate the portfolio sorting exercise above. Specifically, we use close-to-close daily returns of S&P500 Index stocks and compute the cross-sectional tail index each day based on data in the past 22 days[6]. We then compute the tail innovations and do the portfolio sorting same as before. Table 9 reports the performance of the portfolios sorted on betas to shocks in daily return tails, $DailyJ$.

In summary, we see that portfolio sorting result based on daily data share the same trend as the one sorted using shocks to systematic jumps innovations obtained from high-frequency data, that is, there is a decreasing trend in the quintile portfolios. Specifically, the equal-weighted LmH_{DailyJ} portfolio has an annualized return of 6.59% with a t-statistic of 2.3 (annualized SR is 0.54), while the value-weighted LmH_{DailyJ} portfolio has an annualized return of 5.63% with a t-statistic of 3.04, or a SR of 0.71. When test against various factor models, the abnormal returns are most statistically significant, except the models with CiV factors.

[6]We have also tried the estimation using 44/66 days, and perform portfolio sorting based on left or right tails. The results are qualitatively the same.

Table 9: Returns of daily jump tail shock beta-sorted portfolios. Daily jump tails are estimated using a rolling window of 22 days.

		Equal-weight		**Value-weight**	
		Panel A: Mean Portfolio Returns			
Portfolio	**Beta**	**Ret**	**t-stat**	**Ret**	**t-stat**
H	0.13	9.01	4.48	9.23	3.60
Q4	-0.07	12.18	4.19	12.59	3.46
Q3	-0.18	13.80	4.30	14.22	3.52
Q2	-0.28	15.41	4.61	15.17	3.78
L	-0.51	16.51	5.35	14.85	4.77
LmH_{DailyJ}	6.59	2.30	5.63	3.04	
		Panel B: Abnormal Return of LmH_{DailyJ} Portfolio			
Measure		**Ret**	**t-stat**	**Ret**	**t-stat**
CAPM alpha		4.55	2.23	2.53	0.92
FF3 alpha		5.82	3.03	4.51	1.89
FF5 alpha		5.62	3.13	5.65	2.42
FF6 alpha		6.29	3.55	6.41	2.83
CAPM+tailrisk alpha		5.93	2.82	4.82	1.81
FF6+tailrisk alpha		6.52	3.62	6.56	2.85
CAPM+CiV alpha		2.46	1.11	0.72	0.25
FF6+CiV alpha		3.31	1.51	2.69	0.98
CAPM+idiorisk alpha		6.11	2.98	5.08	1.89
FF6+idiorisk alpha		6.43	3.55	6.23	2.69

7 Conclusion

We develop a framework to estimate cross-sectional tail dispersion risks, which are captured by the power-law shape index for the jump tails. The estimators are constructed using high-frequency data from a large cross-section of assets. We prove

asymptotic normality for the tail shape index estimators and propose a goodness-of-fit test for the adequacy of the power law for capturing the systematic and idiosyncratic jump tails, respectively. Empirically, we find that both of these tail dispersion risk factors evolve differently from the concurrent return volatilities. Furthermore, the systematic and idiosyncratic jump tails exhibit distinct time-series dynamics and both carry significant risk premiums, but with opposite signs. The pricing effect of these jump tail dispersion risks cannot be rationalized through their interaction and they remain significant when we control for a number of popular cross-sectional factor pricing models.

Table 10: Returns of shock beta-sorted portfolios for cross-sectional volatility at the presence of systematic jumps.

		Equal-weight		**Value-weight**	
		Panel A: Mean Portfolio Returns			
Portfolio	**Beta**	**Ret**	**t-stat**	**Ret**	**t-stat**
H	1.73	11.24	2.89	10.02	2.99
Q4	0.55	12.32	3.36	10.62	3.65
Q3	0.04	13.07	3.47	13.89	4.76
Q2	-0.48	15.42	3.80	16.89	4.99
L	-1.63	15.81	3.32	16.89	4.00
$\text{LmH}_{CSVol^{SysJ}}$		4.57	2.05	6.88	2.51
		Panel B: Abnormal Return of $\text{LmH}_{CSVol^{SysJ}}$ Portfolio			
Measure		**Ret**	**t-stat**	**Ret**	**t-stat**
CAPM alpha		1.68	0.88	3.44	1.45
FF3 alpha		2.22	1.17	4.06	1.71
FF5 alpha		2.40	1.24	3.93	1.64
FF6 alpha		3.53	2.02	5.16	2.34
CAPM+tailrisk alpha		2.27	1.15	5.08	2.14
FF6+tailrisk alpha		3.62	2.05	5.60	2.57
CAPM+CiV alpha		2.57	1.18	5.58	2.09
FF6+CiV alpha		4.04	1.85	6.30	2.34
CAPM+idiorisk alpha		3.42	1.52	6.18	2.44
FF6+idiorisk alpha		4.02	2.28	6.01	2.83
CAPM+$\text{LmH}_{CSVol^{IdioJ}}$ alpha		2.42	1.23	4.15	1.84
FF6+$\text{LmH}_{CSVol^{IdioJ}}$ alpha		3.71	2.13	5.60	2.57

Table 11: Returns of shock beta-sorted portfolios for cross-sectional volatility when systematic jumps are absent.

		Equal-weight		**Value-weight**	
		Panel A: Mean Portfolio Returns			
Portfolio	**Beta**	**Ret**	**t-stat**	**Ret**	**t-stat**
H	-0.13	12.54	3.98	11.29	4.63
Q4	-0.26	13.62	3.97	13.27	4.68
Q3	-0.43	13.36	3.48	13.29	4.19
Q2	-0.62	13.97	3.24	15.11	4.18
L	-1.06	14.67	2.72	17.09	3.43
$\text{LmH}_{CSVol^{IdioJ}}$		2.13	0.73	5.80	1.62
		Panel B: Abnormal Return of $\text{LmH}_{CSVol^{IdioJ}}$ Portfolio			
Measure		**Ret**	**t-stat**	**Ret**	**t-stat**
CAPM alpha		4.45	2.09	1.88	0.68
FF3 alpha		3.42	1.59	0.79	0.29
FF5 alpha		2.36	1.12	1.26	0.47
FF6 alpha		1.72	0.83	1.79	0.66
CAPM+tailrisk alpha		1.90	1.00	1.16	0.49
FF6+tailrisk alpha		1.46	0.79	1.53	0.64
CAPM+CiV alpha		3.95	1.54	2.60	0.83
FF6+CiV alpha		4.11	1.81	2.83	0.99
CAPM+idiorisk alpha		3.21	1.59	2.75	1.17
FF6+idiorisk alpha		1.46	0.79	2.16	0.91
CAPM+$\text{LmH}_{CSVol^{SysJ}}$ alpha		4.68	2.23	2.14	0.75
FF6+$\text{LmH}_{CSVol^{SysJ}}$ alpha		2.22	1.11	1.31	0.46

References

Acemoglu, D., Carvalho, V. M., Ozdaglar, A., and Tahbaz-Salehi, A. (2012). The network origins of aggregate fluctuations. *Econometrica*, 80(5):1977–2016.

Acemoglu, D., Ozdaglar, A., and Tahbaz-Salehi, A. (2017). Microeconomic origins of macroeconomic tail risks. *American Economic Review*, 107(1):54–108.

Aït-Sahalia, Y., Mykland, P. A., and Zhang, L. (2011). Ultra high frequency volatility estimation with dependent microstructure noise. *Journal of Econometrics*, 160(1):160–175.

Andersen, T. G., Bollerslev, T., Diebold, F. X., and Ebens, H. (2001). The distribution of realized stock return volatility. *Journal of financial economics*, 61(1):43–76.

Andersen, T. G., Fusari, N., and Todorov, V. (2015). The risk premia embedded in index options. *Journal of Financial Economics*, 117(3):558–584.

Andersen, T. G., Fusari, N., and Todorov, V. (2020). The pricing of tail risk and the equity premium: Evidence from international option markets. *Journal of Business & Economic Statistics*, 38(3):662–678.

Andersen, T. G., Todorov, V., and Ubukata, M. (2021). Tail risk and return predictability for the japanese equity market. *Journal of Econometrics*, 222(1):344–363.

Ang, A., Hodrick, R. J., Xing, Y., and Zhang, X. (2006). The cross-section of volatility and expected returns. *The Journal of Finance*, 61(1):259–299.

Asness, C. S., Moskowitz, T. J., and Pedersen, L. H. (2013). Value and momentum everywhere. *The Journal of Finance*, 86(3):929–985.

Axtell, R. L. (2001). Zipf distribution of us firm sizes. *Science*, 293(5536):1818–1820.

Bali, T. G., Cakici, N., and Whitelaw, R. F. (2011). Maxing out: Stocks as lotteries and the cross-section of expected returns. *Journal of Financial Economics*, 99(2):427–446.

Barberis, N. and Huang, M. (2008). Stocks as lotteries: The implications of probability weighting for security prices. *American Economic Review*, 98(5):2066–2100.

Barro, R. J. and Jin, T. (2011). On the size distribution of macroeconomic disasters. *Econometrica*, 79(5):1567–1589.

Blau, B. M., Bowles, T. B., and Whitby, R. J. (2016). Gambling preferences, options markets, and volatility. *Journal of Financial and Quantitative Analysis*, 51(2):515–540.

Bollerslev, T., Li, S. Z., and Todorov, V. (2016). Roughing up beta: Continuous versus discontinuous betas and the cross section of expected stock returns. *Journal of Financial Economics*, 120(3):464–490.

Bollerslev, T., Li, S. Z., and Zhao, B. (2020). Good volatility, bad volatility, and the cross section of stock returns. *Journal of Financial and Quantitative Analysis*, 55(3):751–781.

Bollerslev, T. and Todorov, V. (2011). Estimation of jump tails. *Econometrica*, 79(6):1727–1783.

Bollerslev, T., Todorov, V., and Xu, L. (2015). Tail risk premia and return predictability. *Journal of Financial Economics*, 118(1):113–134.

Boloorforoosh, A., Christoffersen, P., Fournier, M., and Gouriéroux, C. (2020). Beta risk in the cross-section of equities. *The Review of Financial Studies*, 33(9):4318–4366.

Boyer, B. H. and Vorkink, K. (2014). Stock options as lotteries. *The Journal of Finance*, 69(4):1485–1527.

Brunnermeier, M. K., Gollier, C., and Parker, J. A. (2007). Optimal beliefs, asset prices, and the preference for skewed returns. *American Economic Review*, 97(2):159–165.

Chen, A. Y. and Zimmermann, T. (2021). Open source cross-sectional asset pricing. *Critical Finance Review, Forthcoming*.

Clauset, A., Shalizi, C. R., and Newman, M. E. (2009). Power-law distributions in empirical data. *SIAM review*, 51(4):661–703.

Cremers, M., Halling, M., and Weinbaum, D. (2015). Aggregate jump and volatility risk in the cross-section of stock returns. *The Journal of Finance*, 70(2):577–614.

Di Giovanni, J. and Levchenko, A. A. (2012). Country size, international trade, and aggregate fluctuations in granular economies. *Journal of Political Economy*, 120(6):1083–1132.

Eeckhout, J. (2004). Gibrat's law for (all) cities. *American Economic Review*, 94(5):1429–1451.

Fama, E. F. (1965). The behavior of stock-market prices. *The Journal of Business*, 38(1):34–105.

Fama, E. F. and French, K. R. (1993). Common risk factors in the returns on stocks and bonds. *Journal of Financial Economics*, 33(1):3–56.

Fama, E. F. and French, K. R. (2015). A five-factor asset pricing model. *Journal of Financial Economics*, 116(1):1–22.

Fama, E. F. and French, K. R. (2018). Choosing factors. *Journal of Financial Economics*, 128(2):234–252.

Filippou, I., Garcia-Ares, P. A., and Zapatero, F. (2018). Demand for lotteries: The choice between stocks and options. *Available at SSRN 3016462*.

Gabaix, X. (1999). Zipf's law and the growth of cities. *American Economic Review*, 89(2):129–132.

Gabaix, X. (2011). The granular origins of aggregate fluctuations. *Econometrica*, 79(3):733–772.

Gabaix, X. (2012). Variable rare disasters: An exactly solved framework for ten puzzles in macro-finance. *The Quarterly Journal of Economics*, 127(2):645–700.

Gabaix, X., Gopikrishnan, P., Plerou, V., and Stanley, H. E. (2003). A theory of power-law distributions in financial market fluctuations. *Nature*, 423(6937):267–270.

Gabaix, X., Gopikrishnan, P., Plerou, V., and Stanley, H. E. (2006). Institutional investors and stock market volatility. *The Quarterly Journal of Economics*, 121(2):461–504.

Gagliardini, P., Ossola, E., and Scaillet, O. (2016). Time-varying risk premium in large cross-sectional equity data sets. *Econometrica*, 84(3):985–1046.

Gopikrishnan, P., Plerou, V., Amaral, L. A. N., Meyer, M., and Stanley, H. E. (1999). Scaling of the distribution of fluctuations of financial market indices. *Physical Review E*, 60(5):5305.

Gopikrishnan, P., Plerou, V., Gabaix, X., and Stanley, H. E. (2000). Statistical properties of share volume traded in financial markets. *Physical Review E*, 62(4):R4493.

Herskovic, B., Kelly, B., Lustig, H., and Van Nieuwerburgh, S. (2016). The common factor in idiosyncratic volatility: Quantitative asset pricing implications. *Journal of Financial Economics*, 119(2):249–283.

Jacod, J., Lin, H., and Todorov, V. (2024). Systematic jump risk. *Annals of Applied Probability, forthcoming*.

Kelly, B. and Jiang, H. (2014). Tail risk and asset prices. *The Review of Financial Studies*, 27(10):2841–2871.

Kingsley Zipf, G. (1932). *Selected studies of the principle of relative frequency in language*. Harvard university press.

Lin, H. and Todorov, V. (2019). Aggregate asymmetry in idiosyncratic jump risk. *Unpublished manuscript, Northwestern University*.

Mandelbrot, B. (1963). The variation of certain speculative prices. *The Journal of Business*, 36(4):394–419.

Newey, W. K. and West, K. D. (1987). A simple, positive semi-definite, heteroskedasticity and autocorrelation consistent covariance matrix. *Econometrica (1986-1998)*, 55(3):703.

Okuyama, K., Takayasu, M., and Takayasu, H. (1999). Zipf's law in income distribution of companies. *Physica A: Statistical Mechanics and its Applications*, 269(1):125–131.

Smith, R. L. (1987). Estimating tails of probability distributions. *The Annals of Statistics*, pages 1174–1207.

Solnik, B., Boucrelle, C., and Le Fur, Y. (1996). International market correlation and volatility. *Financial Analysts Journal*, 52(5):17–34.

Appendix A Systematic Jump Detection

TRUNC I set daily threshold level to be $\tau_t = 4 \times \Delta_n^{0.49}\sqrt{\min(RV_t, BV_t)}$, where RV_t is daily realized variance $RV = \sum_{j=1}^{n} R_{t,j}^2$, and $BV_t = \pi n/(2(n-1))\sum_{j=1}^{n-1}|R_{t,j}R_{t,j+1}|$, and $R_{t,j}$ is the jth high-frequency return on day t.

TRUNC II set the jump time as $\tau^i = \{(t-1)n + j : |R_{t,j}| > \tau_t, j = 1, ..., 1/\Delta_n\}$.

For type (b) systematic jump, we first get cross-sectional average of returns $\Delta_i^n\overline{P}$, we then apply the same truncation method above by replacing the $R_{t,j}$ with $\Delta_i^n\overline{P}$. Denote the systematic jump time of type (b) as $\tau^{(b)}$.

The type (c) systematic jumps are obtained by the following steps:

step I get continuous cross-sectional average returns $\Delta_i^n\overline{P}^\tau = \Delta_i^n\overline{P}\mathbf{I}_{i\notin\tau^{(b)}}$.

step II remove component in step I from returns: $r_{ji} = R_{ji} - \Delta_i^n\overline{P}^\tau$, where R_{ji} is the ith high-frequency return of stock j

step III Apply truncation (TRUNC I-II) to r_{ji} and get truncated returns r_{ji}^τ.

step IV Compute an unbiased cross-sectional average of g, that is $\check{a}^\tau(g)_i = \hat{a}^\tau(g)_i - 0.5\hat{a}^\tau(g)_{i-1} - 0.5\hat{a}^\tau(g)_{i+1}$, where $\hat{a}^\tau(g)_i = \overline{g(r_{ji}^\tau)} = \sum_{j=1}^{N} g(r_{ji}^\tau)/N$, and we set function $g(x) = x^2$. We compute the un-truncated averages $\check{a}(g)_i = \hat{a}(g)_i - 0.5\hat{a}^\tau(g)_{i-1} - 0.5\hat{a}(g)_{i+1}$, where $\hat{a}(g)_i = \overline{g(r_{ji})} = \sum_{j=1}^{N} g(r_{ji})/N$.

step V Compute $\widehat{VJ}_t = \sum_{i\Delta_n\in(t,t+1]}|\check{a}^\tau(g)_i|$

step VI Set threshold as $\tau_t^v = \delta \times \Delta_n^{0.98}\widehat{VJ}_t$, $\delta = 12$.

step VII Systematic jump time $\tau^{(c)'} = \{(n-1)t + j : |\hat{a}^\tau(g)_{(n-1)t+j}| \geq \tau_t^v, j = 1, ..., 1/\Delta_n, t = 1, ..., \}$.

step VIII compute cross-sectional average of g^2: $\hat{a}(g^2)_i = \overline{g(r_{ji})^2} = \sum_{j=1}^{N}(g(r_{ji}))^2/N$.

step IX Set threshold as $\tau_i^{v'} = \delta \times \Delta_n^{0.98}\sqrt{\hat{a}(g^2)_i}$.

step X Systematic jump time $\tau^{(c)''} = \{i : |\hat{a}(g)_i| \geq \tau_i^{v'}\}$.

step XI Finally, the systematic jump time of type (c) is set to be $\tau^{(c)} = \tau^{(c)''} \cap \tau^{(c)'}$.

Appendix B Portfolio sorting results with a three-month holding window

In this section, we report the portfolio sorting results for a holding window of three months. In Tables 12, 13 and 14, we summarize the performance of the portfolios sorted using systematic jump risk, idiosyncratic jump risk, and the combined portfolio, respectively. We see that overall the conclusions are qualitatively the same as the portfolio sorting with a one-month holding window.

Table 12: Returns of systematic jump tail innovation beta-sorted portfolios. The holding window of the portfolio is three months (66 days).

Three-month holding window				
	Equal-weight		Value-weight	
	Panel A: Average Return of Portfolios			
Portfolio	Ret	T-stat	Ret	T-stat
H	11.36	2.89	11.31	3.19
Q4	13.13	3.72	10.73	3.80
Q3	13.80	3.94	13.35	5.04
Q2	14.55	4.09	16.20	5.73
L	15.87	3.81	16.25	4.66
LmH_{SysJ}	4.50	2.37	4.93	1.94
	Panel B: Abnormal Return of LmH_{SysJ} Portfolio			
Measure	Ret	T-stat	Ret	T-stat
CAPM alpha	3.68	1.92	4.39	1.58
FF3 alpha	3.77	1.91	4.60	1.60
FF5 alpha	4.79	2.32	6.16	2.26
FF6 alpha	6.10	3.11	7.78	3.02
CAPM+tailrisk alpha	4.83	2.32	7.01	2.61
FF6+tailrisk alpha	6.52	3.23	9.00	3.53
CAPM+CiV alpha	8.92	2.42	8.56	1.87
FF6+CiV alpha	9.30	1.47	8.86	1.17
CAPM+idiorisk alpha	5.87	2.35	7.92	2.56
FF6+idiorisk alpha	6.92	3.40	9.19	3.50
CAPM+HmL_{IdioJ} alpha	3.90	2.18	6.18	2.28
FF6+HmL_{IdioJ} alpha	6.17	3.22	9.35	3.57

Table 13: Returns of idiosyncratic jump tail innovation beta-sorted portfolios. The holding window of the portfolio is three months (66 days).

Three-month holding window				
	Equal-weight		Value-weight	
	Panel A: Average Return of Portfolios			
Portfolio	Ret	T-stat	Ret	T-stat
H	15.29	3.93	15.84	5.00
Q4	14.21	4.10	13.60	5.27
Q3	13.60	3.82	10.92	4.17
Q2	13.27	3.69	11.21	4.04
L	12.54	3.05	12.09	3.54
HmL_{IdioJ}	2.75	1.55	3.76	1.74
	Panel B: Abnormal Return of HmL_{IdioJ} Portfolio			
Measure	Ret	T-stat	Ret	T-stat
CAPM alpha	3.67	1.69	4.40	1.53
FF3 alpha	3.73	1.67	4.11	1.32
FF5 alpha	3.07	1.43	3.80	1.24
FF6 alpha	3.12	1.47	3.67	1.17
CAPM+tailrisk alpha	4.14	1.86	5.26	1.74
FF6+tailrisk alpha	3.80	1.48	4.69	1.52
CAPM+CiV alpha	1.16	0.45	1.80	0.56
FF6+CiV alpha	-0.63	0.20	-1.42	0.39
CAPM+idiorisk alpha	3.61	1.77	4.21	1.66
FF6+idiorisk alpha	3.56	1.81	4.11	1.54
CAPM+LmH_{SysJ} alpha	3.91	1.95	5.01	1.87
FF6+LmH_{SysJ} alpha	3.45	1.87	4.63	1.69

Table 14: Performance of combined portfolio. The holding window is 3 months.

Three-month holding window				
	Equal-weight		Value-weight	
	Panel A: Correlation between SysJ and IdioJ			
Cor(SysJ,IdioJ)	-0.11		-0.07	
	Panel B: Performance of the combined Portfolio			
Measure	Ret	T-stat	Ret	T-stat
MEAN	3.76	3.06	4.24	2.58
CAPM alpha	4.20	2.68	5.04	2.21
FF3 alpha	4.15	2.53	4.92	2.00
FF5 alpha	4.29	2.59	5.58	2.39
FF6 alpha	4.96	3.21	6.35	2.82
CAPM+tailrisk alpha	4.88	2.96	6.77	3.09
FF6+tailrisk alpha	5.48	3.5	7.51	3.42
CAPM+CiV alpha	1.16	0.45	1.80	0.56
FF6+CiV alpha	-0.63	-0.2	-1.42	-0.39
CAPM+idiorisk alpha	5.32	3.05	6.87	3.11
FF6+idiorisk alpha	5.74	3.69	7.46	3.46

Appendix C Portfolio sorting for systematic jump detection with various thresholds

As a robustness check, we evaluate the portfolio sorting results based on systematic jump detection with various threshold parameters. We set the tuning parameter for latent systematic jump detection in steps V and IX to be $\delta = 10$, or 8. The detected systematic jumps are then around 1 for every 5 days and 3.5 days, respectively.

In Tables 15–18, we summarize the portfolio sorting results. We see that the conclusions are qualitatively the same for various thresholding parameters. The quantile portfolios with higher exposure to systematic/idiosyncratic jump innovations have lower/higher returns. In addition, the alphas of the $\text{LmH}_{SysJ}/\text{HmL}_{Idio}$ portfolios sorted by systematic/idiosyncratic jumps exposures are statistically significant after controlling for various factors.

C.1 Portfolio sorting: threshold $\delta = 10$

C.1.1 portfolio sorting based on exposure to systematic jump tail index shocks

Table 15: Returns of systematic jump tail shock beta-sorted portfolios. The holding window of the portfolio is one month. Tuning parameter for systematic jump detection $\delta = 10$.

One-month holding window				
	Equal-weight		Value-weight	
	Panel A: Average Return of Portfolios			
Portfolio	Ret	T-stat	Ret	T-stat
H	11.10	2.68	11.43	3.11
Q4	13.38	3.53	11.85	3.73
Q3	12.87	3.44	12.82	4.43
Q2	14.81	3.75	15.45	4.87
L	15.48	3.49	15.30	4.20
LmH_{SysJ}	4.38	2.36	3.87	1.49
	Panel B: Abnormal Return of LmH_{SysJ} Portfolio			
Measure	Ret	T-stat	Ret	T-stat
CAPM alpha	3.07	1.62	3.1	1.18
FF3 alpha	3.29	1.77	3.76	1.45
FF5 alpha	3.34	1.76	3.46	1.31
FF6 alpha	3.84	2.01	3.99	1.50
CAPM+tailrisk alpha	3.37	1.70	4.12	1.54
FF6+tailrisk alpha	3.81	1.94	4.45	1.65
CAPM+CiV alpha	3.61	1.50	5.43	1.74
FF6+CiV alpha	4.24	1.72	5.63	1.73
CAPM+idiorisk alpha	3.66	1.69	3.91	1.36
FF6+idiorisk alpha	3.99	2.03	4.35	1.60

Table 16: Returns of systematic jump tail shock beta-sorted portfolios. The holding window of the portfolio is three months (66 days). Tuning parameter for systematic jump detection $\delta = 10$.

Three-month holding window				
	Equal-weight		Value-weight	
	Panel A: Average Return of Portfolios			
Portfolio	Ret	T-stat	Ret	T-stat
H	11.74	2.94	12.35	3.36
Q4	13.71	3.88	11.88	4.08
Q3	12.95	3.72	13.32	5.08
Q2	14.81	4.14	15.33	5.27
L	15.41	3.78	15.11	4.52
LmH_{SysJ}	3.68	2.02	2.76	1.01
	Panel B: Abnormal Return of LmH_{SysJ} Portfolio			
Measure	Ret	T-stat	Ret	T-stat
CAPM alpha	3.14	1.61	2.59	0.87
FF3 alpha	3.01	1.46	2.47	0.77
FF5 alpha	3.31	1.62	3.25	1.07
FF6 alpha	4.48	2.24	4.75	1.6
CAPM+tailrisk alpha	3.86	1.84	4.59	1.56
FF6+tailrisk alpha	4.98	2.42	6.16	2.09
CAPM+CiV alpha	7.24	2.25	8.03	1.56
FF6+CiV alpha	6.94	1.29	9.41	1.17
CAPM+idiorisk alpha	4.45	1.8	5.19	1.56
FF6+idiorisk alpha	5.24	2.53	6.47	2.23

C.1.2 portfolio sorting based on exposure to idiosyncratic jump tail index shocks

Table 17: Returns of idiosyncratic jump tail shock beta-sorted portfolios. The holding window of the portfolio is one month. Tuning parameter for systematic jump detection $\delta = 10$.

One-month holding window				
	Equal-weight		Value-weight	
	Panel A: Average Return of Portfolios			
Portfolio	Ret	T-stat	Ret	T-stat
H	15.34	3.81	15.56	4.73
Q4	13.78	3.67	12.85	4.51
Q3	13.46	3.57	10.44	3.59
Q2	13.17	3.37	11.25	3.69
L	12.40	2.74	11.74	3.13
HmL_{IdioJ}	2.94	1.78	3.82	1.79
	Panel B: Abnormal Return of HmL_{IdioJ} Portfolio			
Measure	Ret	T-stat	Ret	T-stat
CAPM alpha	4.33	2.27	5.28	2.12
FF3 alpha	4.05	2.07	4.53	1.77
FF5 alpha	4.26	2.16	4.84	1.84
FF6 alpha	4.18	2.13	4.71	1.80
CAPM+tailrisk alpha	4.73	2.45	6.21	2.48
FF6+tailrisk alpha	4.73	2.40	5.69	2.17
CAPM+CiV alpha	4.07	1.98	5.86	2.5
FF6+CiV alpha	4.32	2.09	6.13	2.51
CAPM+idiorisk alpha	4.09	2.22	4.95	2.14
FF6+idiorisk alpha	4.43	2.32	5.03	2.07

Table 18: Returns of idiosyncratic jump tail innovation beta-sorted portfolios. The holding window of the portfolio is three months (66 days). Tuning parameter for systematic jump detection $\delta = 10$.

Three-month holding window				
	Equal-weight		Value-weight	
	Panel A: Average Return of Portfolios			
Portfolio	Ret	T-stat	Ret	T-stat
H	15.15	3.99	15.85	5.11
Q4	14.10	4.1	13.12	5.18
Q3	13.61	3.89	10.82	4.07
Q2	13.39	3.62	11.49	4.10
L	12.69	3.04	11.91	3.36
HmL_{IdioJ}	2.46	1.36	3.95	1.76
	Panel B: Abnormal Return of HmL_{IdioJ} Portfolio			
Measure	Ret	T-stat	Ret	T-stat
CAPM alpha	3.79	1.67	5.26	1.78
FF3 alpha	3.77	1.58	4.91	1.51
FF5 alpha	3.35	1.46	4.78	1.49
FF6 alpha	3.37	1.47	4.64	1.42
CAPM+tailrisk alpha	4.45	1.93	6.13	2.01
FF6+tailrisk alpha	4.19	1.90	5.57	1.73
CAPM+CiV alpha	0.73	0.27	2.01	0.65
FF6+CiV alpha	-1.53	0.46	-1.57	0.40
CAPM+idiorisk alpha	3.89	1.87	5.11	1.98
FF6+idiorisk alpha	3.88	1.89	4.93	1.80

C.2 Portfolio sorting: threshold $\delta = 8$

C.2.1 Portfolio sorting based on exposure to systematic jump tail index shocks

Table 19: Returns of systematic jump tail shock beta-sorted portfolios. The holding window of the portfolio is one month. Tuning parameter for systematic jump detection $\delta = 8$.

One-month holding window				
	Equal-weight		Value-weight	
	Panel A: Average Return of Portfolios			
Portfolio	Ret	T-stat	Ret	T-stat
H	9.95	2.43	10.80	2.96
Q4	12.55	3.29	11.13	3.40
Q3	13.47	3.57	12.94	4.44
Q2	15.24	3.90	14.64	4.60
L	16.60	3.70	16.38	4.43
LmH_{SysJ}	6.65	3.25	5.58	2.08
	Panel B: Abnormal Return of LmH_{SysJ} Portfolio			
Measure	Ret	T-stat	Ret	T-stat
CAPM alpha	5.27	2.57	5.07	1.84
FF3 alpha	5.69	2.84	5.85	2.14
FF5 alpha	5.55	2.69	5.51	1.91
FF6 alpha	6.17	3.01	6.24	2.17
CAPM+tailrisk alpha	5.77	2.67	5.79	2.03
FF6+tailrisk alpha	6.24	2.98	6.45	2.21
CAPM+CiV alpha	5.73	2.22	7.29	2.00
FF6+CiV alpha	5.52	2.09	6.15	1.64
CAPM+idiorisk alpha	6.35	2.75	6.40	2.12
FF6+idiorisk alpha	6.54	3.12	6.70	2.29

Table 20: Returns of systematic jump tail innovation beta-sorted portfolios. The holding window of the portfolio is three months (66 days). Tuning parameter for systematic jump detection $\delta = 8$.

Three-month holding window				
	Equal-weight		Value-weight	
	Panel A: Average Return of Portfolios			
Portfolio	Ret	T-stat	Ret	T-stat
H	10.88	2.82	11.74	3.31
Q4	12.69	3.55	11.20	3.79
Q3	13.79	3.99	13.5	5.17
Q2	15.11	4.18	14.46	4.82
L	16.37	3.96	16.25	4.83
LmH_{SysJ}	5.49	2.88	4.51	1.76
	Panel B: Abnormal Return of LmH_{SysJ} Portfolio			
Measure	Ret	T-stat	Ret	T-stat
CAPM alpha	4.45	1.95	4.18	1.42
FF3 alpha	4.47	1.91	4.27	1.40
FF5 alpha	4.61	1.93	5.2	1.75
FF6 alpha	5.89	2.59	6.78	2.38
CAPM+tailrisk alpha	5.36	2.22	5.88	2.05
FF6+tailrisk alpha	6.58	2.81	7.83	2.77
CAPM+CiV alpha	9.31	2.52	8.01	1.59
FF6+CiV alpha	7.64	1.29	6.27	0.74
CAPM+idiorisk alpha	6.35	2.42	7.47	2.43
FF6+idiorisk alpha	7.01	3.08	8.51	3.11

C.2.2 Portfolio sorting based on exposure to idiosyncratic jump tail index shocks

Table 21: Returns of idiosyncratic jump tail shock beta-sorted portfolios. The holding window of the portfolio is one month. Tuning parameter for systematic jump detection $\delta = 8$.

One-month holding window				
	Equal-weight		Value-weight	
	Panel A: Average Return of Portfolios			
Portfolio	Ret	T-stat	Ret	T-stat
H	15.52	3.85	15.55	4.59
Q4	12.73	3.34	10.3	3.64
Q3	14.13	3.77	13.64	4.83
Q2	13.34	3.42	10.97	3.59
L	12.25	2.73	11.11	2.95
HmL_{IdioJ}	3.27	1.96	4.44	2.02
	Panel B: Abnormal Return of HmL_{IdioJ} Portfolio			
Measure	Ret	T-stat	Ret	T-stat
CAPM alpha	4.55	2.36	5.73	2.15
FF3 alpha	4.29	2.15	4.96	1.80
FF5 alpha	4.44	2.21	5.27	1.85
FF6 alpha	4.28	2.15	5	1.77
CAPM+tailrisk alpha	4.76	2.41	6.62	2.42
FF6+tailrisk alpha	4.69	2.34	5.94	2.10
CAPM+CiV alpha	4.96	2.37	6.28	2.57
FF6+CiV alpha	4.81	2.29	5.65	2.18
CAPM+idiorisk alpha	4.46	2.38	5.94	2.40
FF6+idiorisk alpha	4.6	2.37	5.73	2.17

Table 22: Returns of idiosyncratic jump tail innovation beta-sorted portfolios. The holding window of the portfolio is three months (66 days). Tuning parameter for systematic jump detection $\delta = 8$.

Three-month holding window				
	Equal-weight		Value-weight	
	Panel A: Average Return of Portfolios			
Portfolio	Ret	T-stat	Ret	T-stat
H	15.44	4.04	16.15	2.26
Q4	13.04	3.67	10.76	1.86
Q3	14.28	4.18	13.5	1.83
Q2	13.57	3.73	11.07	1.92
L	12.58	3.00	11.75	2.37
HmL_{IdioJ}	2.86	1.57	4.4	1.54
	Panel B: Abnormal Return of HmL_{IdioJ} Portfolio			
Measure	Ret	T-stat	Ret	T-stat
CAPM alpha	4.17	1.85	5.50	1.80
FF3 alpha	4.16	1.76	5.10	1.53
FF5 alpha	3.63	1.62	4.69	1.45
FF6 alpha	3.62	1.61	4.49	1.34
CAPM+tailrisk alpha	4.70	2.06	6.49	2.07
FF6+tailrisk alpha	4.24	1.96	5.44	1.66
CAPM+CiV alpha	0.84	0.30	2.13	0.65
FF6+CiV alpha	-2.03	0.54	-2.45	0.52
CAPM+idiorisk alpha	4.33	2.07	5.58	2.08
FF6+idiorisk alpha	4.02	1.97	4.96	1.75

Appendix D Assumptions

In this section, we state the assumptions needed for our theoretical results. First, the systematic jump process $\{J_{it}\}$ is given by

$$J_{it} = \sum_{q \geq 1} \lambda_{iq} \mathbf{1}_{\{\rho_q \leq t\}}, \tag{D.1}$$

where $(\rho_p)_{p\geq 1}$ is a strictly increasing sequence of positive stopping times going to ∞, capturing the timing of the systematic jumps in asset prices, and λ_{iq} capture the size of the systematic jumps.

The idiosyncratic jumps in the asset prices have the following representation

$$\widetilde{J}_{it} = \int_0^t \int_{\mathbb{R}_+} \int_{\mathbb{R}} \left(1_{\{u<\varphi_{it}^-,\, z<0\}} + 1_{\{u>\varphi_{it}^+,\, z>0\}}\right) z \mu_i(ds, du, dz), \tag{D.2}$$

where $(\mu_i)_{i\geq 1}$ is a sequence of independent Poisson measures on $\mathbb{R}_+ \times \mathbb{R}_+ \times \mathbb{R}$ with compensator $ds \otimes du \otimes \nu(z)dz$, for some nonnegative measure ν; $\{\varphi_{it}^{\pm}\}$ are some predictable processes. The second dimension of the Poisson measure is used for thinning and generates time-varying intensity of jumps, which can differ depending on their sign. Indeed, an alternative (and equivalent) representation for $\{\widetilde{J}_{it}\}$ is as a jump process with jump compensator on $\mathbb{R}_+ \times \mathbb{R}$ (the first dimension capturing time and the second one the jump size) being $(\varphi_{it}^- 1_{\{z<0\}}) + \varphi_{it}^+ 1_{\{z>0\}}))dt \otimes d\nu(z)$.

We next define formally the set of indices of the high-frequency increments containing the systematic jumps that is denoted by T_n. It is given by

$$T_n = \{i : ((i-1)\Delta_n, i\Delta_n] \text{ contains a } \rho_p, i = 1, .., n\}.$$

We let $\widehat{T}_n$ denote an estimator of this set. The following assumption formalizes the sense in which $\widehat{T}_n$ is consistent for T_n,

Assumption 1 (Systematic Jump Time Estimation) *The set T_n is finite almost surely. In addition, as $N \to \infty$ and $n \to \infty$,*

$$\mathbb{P}(\widehat{T}_n = T_n) \to 1.$$

As we already mentioned, this assumption is satisfied by the method of systematic jump identification used in Jacod et al. (2024), which we also use for our application.

Our next assumption concerns the cross-sectional dependence of various quantities that appear in the definitions of the jumps. We are interested in the cross-sectional dependence conditional on the common shocks σ-algebra $\mathcal{C}$ that contains various aggregate level shocks. In particular, the stopping times $(\rho_p)_{p\geq 1}$, the vector of sys-

tematic Brownian motions $\mathbf{W}_t$, the measure ν, and more generally any economy-wide (systematic) shocks are all adapted to $\mathcal{C}$. Our assumption is then as follows,

Assumption 2 ($\mathcal{C}$-conditional Independence) *Conditional on $\mathcal{C}$:*

(a) λ_{ip} is independent from $\lambda_{i'p'}$ if $(i,p) \neq (i',p')$,

(b) the processes $(\varphi_{it}^{\pm})$ are independent for different values of i,

(c) the sequence $(\lambda_{ip})_{\{p\geq 1\}}$ is independent from the processes $(\varphi_{i't}^{\pm})$ if $i \neq i'$.

We note that the cross-sectional independence needs to apply only after conditioning on $\mathcal{C}$. Therefore, we can allow for common factors to drive the systematic jumps or the idiosyncratic jump intensities.

We turn next to the assumptions concerning the regular variation of the jump tails. For a unction $g : \mathbb{R} \to \mathbb{R}$, our generic assumption for regular variation in the tails of $g_{\psi}^{\pm}(x)$ is given by,

Assumption RegV *For a function $g : \mathbb{R} \to \mathbb{R}$, $\overline{g}_{\psi}^{\pm}(x)$ are regularly varying with index $1/\xi^{\pm} > 0$, that is,*

$$\lim_{x\to\infty} \frac{\overline{g}_{\psi}^{\pm}(\delta x)}{\overline{g}_{\psi}^{\pm}(x)} = \delta^{-1/\xi^{\pm}}, \text{ for all } \delta > 0.$$

Moreover,

$$\lim_{x\to\infty} \frac{\delta^{1/\xi^{\pm}}\overline{g}_{\psi}^{\pm}(\delta x)}{\overline{g}_{\psi}^{\pm}(x)} = 1 + O(\tau^{\pm}(x)), \text{ for all } \delta > 0,$$

where $\tau^{\pm}(x) > 0$, $\tau^{\pm}(x) \to 0$ as $x \uparrow \infty$, and $\tau^{\pm}(x)$ are non-increasing.

This assumption means that the tails of $g_{\psi}^{\pm}(x)$ can be approximated by a power function. The parameters $\xi^{\pm}$ capture the rate of tail decay and play a key role in describing the tail behavior. We impose regular variation for the tails of systematic and idiosyncratic jumps in the following two assumptions,

Assumption 3 (Systematic Jump Tails) *Conditional on $\mathcal{C}$, $(\lambda_{ip})_{1\leq i\leq N}$ is an i.i.d. sequence of random variables with probability density function $f_p(x)$, for $p = 1, 2, ...$*

Each $f_p(x)$ satisfies Assumption RegV with the same $\xi^{\pm} = \xi_S^{\pm}$ and $\tau^{\pm} = \tau_S^{\pm}$, for $\xi_S^{\pm}$ being some $\mathcal{C}$-adapted random variables and $\tau_S^{\pm}$ being some $\mathcal{C}$-adapted functions.

Assumption 4 (Idiosyncratic Jump Tails) *The jump density measure $\nu(x)$ is $\mathcal{C}$-adapted and satisfies Assumption RegV with $\xi^{\pm} = \xi_I^{\pm}$ and $\tau = \tau_I^{\pm}$, for $\xi_I^{\pm}$ being some $\mathcal{C}$-adapted random variables and $\tau_I^{\pm}$ being some $\mathcal{C}$-adapted functions.*

We note that in the above assumptions, $\xi_S^{\pm}$ and $\xi_I^{\pm}$ are random variables (adapted to $\mathcal{C}$). This is important because the tail decay parameters vary significantly over time empirically.

Finally, for deriving the behavior of our tail estimators, we need some relatively mild assumptions related to existence of moments of certain variables appearing in the asset price dynamics as well as some smoothness in expectations. They are collected in the following assumption,

Assumption 5 ($\mathcal{C}$-conditional Moments) *There is a sequence $T_1, T_2, ...$ of stopping times increasing to ∞ such that for all $i \geq 1$, $0 \leq s \leq t < T_m$ and $p \geq 2$:*

$$\mathbb{E}\left(\left(\sup_{t' \in [s,t]} |\varphi_{it}^{\pm} - \varphi_{it'}^{\pm}| \right)^p \middle| \mathcal{C} \right) < K_p |t - s|, \tag{D.3}$$

and

$$\mathbb{E}\left(\left(\varphi_{it}^{\pm} + |\alpha_{it}| + \widetilde{\sigma}_{it}^2 + \|\boldsymbol{\beta}_{i,t}\|^2 \right)^p \middle| \mathcal{C} \right) < K_p, \tag{D.4}$$

for some $\mathcal{C}$-adapted random variable $K_p > 0$.

Condition (D.3) is satisfied if $\varphi_{it}^{\pm}$ follows an Ito semimartingale, which is the standard approach to modeling the continuous-time dynamics in economics. Conditions (D.4) all concern the existence of conditional moments. They are much weaker than requiring the existence of unconditional moments.

Finally, for the estimators of $\xi_S^{\pm}$ and $\xi_I^{\pm}$, we need rate conditions involving N, Δ_n and the residual functions $\tau^{\pm}$. These are given in the following two conditions:

Conditions SJ *Suppose $p \geq 1$, and as $N \to \infty$, $\Delta_n \to 0$, and $\rho_N^S \to \infty$, assume that $\inf_{p \geq 1} N \bar{f}_{p,\psi}^{+}(\rho_N^S) \to \infty$, $\sup_{p \geq 1} \sqrt{N \bar{f}_{p,\psi}^{+}(\rho_N^S)} \tau^{+}(\rho_N^S) \to 0$,*

$\sup_{p\geq 1} \Delta_n \overline{\nu}^+_\psi(\rho^S_N)\sqrt{N/\overline{f}_{p,\psi^+}(\rho^S_N)} \to 0$, *and*

$$\sqrt{N\Big(\sup_{p\geq 1} \bar{f}^+_{p,\psi}(\rho^S_N)\Big)\Delta_n^{3-\varepsilon}}\left(1 \bigvee \frac{\sqrt{\Delta_n}}{\inf_{p\geq 1} \bar{f}^+_{p,\psi}(\rho^S_N)}\right) \to 0, \quad \text{for some } \varepsilon > 0. \tag{D.5}$$

Conditions IJ *As* $N \to \infty$, $\Delta_n \to 0$, *and* $\rho^I_N \to \infty$, *assume* $N\,\overline{\nu}^+_\psi(\rho^I_N) \to \infty$, $\sqrt{N\,\overline{\nu}^+_\psi(\rho^I_N)}\;\tau^+(\rho^I_N) \to 0$, *and for some* $\varepsilon > 0$,

$$\sqrt{N\,\overline{\nu}^+_\psi(\rho^I_N)\,\Delta_n^{1-\varepsilon}}\left(1 \bigvee \frac{\sqrt{\Delta_n}}{\overline{\nu}^+_\psi(\rho^I_N)}\right) \;\to\; 0. \tag{D.6}$$

Appendix E Goodness-of-Fit Test Definitions

We define the limiting variables $\mathcal{K}^{S+}$ and $\mathcal{K}^{I+}$ formally in this section. We start with the former. We let X^S_N denote an infeasible KS statistic computed using a sample of random variables of size $N\overline{f}^+_\psi(\rho^S_N)$, that follow the power law with tail decay parameter ξ^+_S and location ρ^S_N, along with the power law distribution with a tail decay parameter obtained via maximum likelihood estimation (MLE). Specifically, suppose that $(x_i)_{i=1,\ldots,[N\overline{f}^+_\psi(\rho^S_N)]}$ are i.i.d. drawn from the Pareto distribution with tail probability $(x/\rho^S_N)^{-1/\xi^+_S}$ for $x \geq \rho^S_N$. Then,

$$X^S_N \;\sim\; \sup_x \left| \sum_{i=1}^{[N\overline{f}^+_\psi(\rho^S_N)]} \frac{1}{N\overline{f}^+_\psi(\rho^S_N)} \mathbf{1}_{\{x_i > x\}} - \left(\frac{x}{\rho^S_N}\right)^{-1/\widetilde{\xi}^+_S} \right|, \qquad \text{for } x \geq \rho^S_N\,,$$

where $\widetilde{\xi}^+_S = \sum_{i=1}^{[N\overline{f}^+_\psi(\rho^S_N)]} \log(x_i/\rho^S_N)/[N\overline{f}^+_\psi(\rho^S_N)]$ is the MLE based on $(x_i)_{i=1,\ldots,[N\overline{f}^+_\psi(\rho^S_N)]}$.

Further, we let the limiting distribution of $\sqrt{N\overline{f}^+_\psi(\rho^S_N)}X^S_N$ be denoted $\mathcal{K}^{S+}$, i.e.,

$$\sqrt{N\overline{f}^+_\psi(\rho^S_N)}X^S_N \;\overset{\mathcal{L}|\mathcal{C}}{\to}\; \mathcal{K}^{S+}, \quad \text{as} \quad N\overline{f}^+_\psi(\rho^S_N) \to \infty\,.$$

When using the fitted Pareto distribution in the KS statistic, $\mathcal{K}^{S+}$ does not have a closed-form expression. Simulation can be used, instead, for estimating its quantiles, as done by Clauset et al. (2009).

We continue next with $\mathcal{K}^{I+}$. We let X_N^I denote an infeasible KS statistic computed using a sample of size $\sum_{i=1}^N \overline{\nu}_\psi^+(\rho_N^I)\mathbb{E}\Big(\int_0^1 \varphi_{it}^+ dt\Big)$ that follows the power law with tail decay parameter ξ_I^+ and location ρ_N^I. Write $\mathcal{K}^{I+}$ as the limiting distribution of $\sqrt{\sum_{i=1}^N \overline{\nu}_\psi^+(\rho_N^I)\mathbb{E}\Big(\int_0^1 \varphi_{it}^+ dt\Big)}X_N^I$, i.e.,

$$\sqrt{\sum_{i=1}^N \overline{\nu}_\psi^+(\rho_N^I)\,\mathbb{E}\Big(\int_0^1 \varphi_{it}^+ dt\Big)}\; X_N^I \xrightarrow{\mathcal{L}|\mathcal{C}} \mathcal{K}^{I+}, \quad \text{as } N\,\overline{\nu}_\psi^+(\rho_N^I) \to \infty\,.$$

Appendix F Goodness-of-Fit for Cross-Sectional Idiosyncratic Return Tails

We next proceed to the goodness-of-fit test for the power law characterization of the idiosyncratic jump tails. The corresponding KS statistic is given by,

$$D_N^I = \sup_x |\, F_N^I(x) - P_N^I(x)\,|\,, \tag{F.1}$$

where $F_N^I(x)$ is the empirical tail distribution for the idiosyncratic jumps,

$$F_N^I(x) = \frac{1}{\widehat{M}_N^{I+}} \sum_{i=1}^N \sum_{j\in\widehat{T}_n^c} \mathbf{1}_{\{\psi^+(\Delta_j^n p_i)>x\}}, \quad \text{for } x \geq \rho_N^I, \tag{F.2}$$

and $P_N^I(x)$ is the tail probability of the estimated Pareto distribution,

$$P_N^I(x) = \left(\frac{x}{\widehat{M}_N^{I+}}\right)^{-1/\widehat{\xi}_I^+}, \quad \text{for } x \geq \rho_N^I, \tag{F.3}$$

and $\widehat{\xi}_I^+$ and $\widehat{M}_N^{I+}$ are defined in equations (3.4) and (3.5), respectively.

We have the following result about the KS statistic.

Theorem 4 *Suppose the assumptions of Theorem 2 apply with $\tau_I^+(x) \equiv 0$ for all $x \geq \rho_N^I$. Then,*

$$\sqrt{\widehat{M}_N^{I+}}\, D_{N,t}^I \xrightarrow{\mathcal{L}|\mathcal{C}} \mathcal{K}^{I+},$$

where $\mathcal{K}^{I+}$ is defined in Appendix E.

Theorem 4 suggests that the asymptotic distribution of the proposed KS statistic is identical to that of the KS statistic based on data generate by the exact power law. As in the case of the systematic jump tails, the quantiles of $\mathcal{K}^{I+}$ can be easily estimated via simulation.

Appendix G Proofs

Denote the score associated with the log-likelihood of the power law distribution by

$$\phi^+(u,\xi^+) = \log(\xi^+) + \left(1+\frac{1}{\xi^+}\right)\log\left(1+\frac{u}{x}\right).$$

We can define an infeasible estimator of ξ_I^+ based on direct observation of the idiosyncratic jumps. More specifically, we define

$$g_N^I(\xi^+,\rho_N^I) = \frac{1}{M_N^{I+}}\left(\sum_{i=1}^N\int_0^1\int_{\mathbb{R}}\phi^+(\psi^+(x)-\rho_N^I,\xi^+)\mathbf{1}_{\{\psi^+(x)>\rho_N^I\}}\mu_i(ds,dx)\right),$$

where M_N^{I+} denotes the total number of positive idiosyncratic jumps for all stocks over the time interval $[0,1]$ that exceed ρ_N^I upon transformation by $\psi^+(\cdot)$. That is,

$$M_N^{I+} = \sum_{i=1}^N\int_0^1\int_{\mathbb{R}}\mathbf{1}_{\{\psi^+(x)>\rho_N^I\}}\mu_i(ds,dx). \tag{G.1}$$

By setting $g_N^I(\xi^+,\rho_N) = 0$, we get the MLE, or Hill's estimator of idiosyncratic jump tail parameter,

$$\widetilde{\xi_I}^+ = \frac{1}{M_N^{I+}}\left(\sum_{i=1}^N\int_0^1\int_{\mathbb{R}}\log\left(\frac{\psi^+(x)}{\rho_N^I}\right)\mathbf{1}_{\{\psi^+(x)>\rho_N^I\}}\mu_i(ds,dx)\right). \tag{G.2}$$

Similarly, for systematic jumps, we have the infeasible MLE based on direct ob-

servations of the systematic jumps,

$$\widetilde{\xi_S}^+ = \frac{1}{M_N^{S+}} \left(\sum_{i=1}^{N} \sum_{p \geq 1} \log \left(\frac{\psi^+(\lambda_{ip})}{\rho_N^S} \right) \right), \tag{G.3}$$

where M_N^{S+} denotes the total number of positive systematic jumps for all stocks over the interval $[0, 1]$ that exceed ρ_N^S upon transformation by $\psi(\cdot)$. That is

$$M_N^{S+} = \sum_{i=1}^{N} \sum_{p \geq 1} \int_{\mathbb{R}} \mathbf{1}_{\{\psi^+(\lambda_{ip}) > \rho_N^S\}}. \tag{G.4}$$

The following results are about the estimators above using the infeasible stock jumps. We have the following lemmas.

Lemma 1 *For the process* $\{p_{it}\}$ *defined in* (2.1)*, assume Assumptions 2 and 4, for all* $i \geq 1$*, there exists* $K > 0$*,* $\iota < 1$*,* $0 < \mathbb{E}(\varphi_{it}^+)^{2(1+\iota)} < K$*, in addition,* $N \to \infty$*,* $\rho_N^I \to \infty$*,* $N\overline{\nu}_\psi^+(\rho_N^I) \to \infty$*, and* $\sqrt{N\overline{\nu}_\psi^+(\rho_N^I)}\tau_I^+(\rho_N^I) \to 0$ *as* $N \to \infty$*. Then*

$$\sqrt{M_N^{I+}}(\widetilde{\xi_I}^+ - \xi_I^+) \xrightarrow{\mathcal{L}|\mathcal{C}} N\big(0, (\xi_I^+)^2\big). \tag{G.5}$$

Proof:

First, for an integer k, by a change of variable of integration,

$$\begin{aligned} &\int_{\mathbb{R}} \left(\log \left(\frac{\psi^+(x)}{\rho_N^I} \right) \right)^k \mathbf{1}_{\{\psi^+(x) > \rho_N^I\}} \nu(x) dx \\ =&\overline{\nu}_\psi^+(\rho_N^I) \int_0^\infty \left(\log \left(1 + \frac{u}{\rho_N^I} \right) \right)^k \left(1 - \frac{\overline{\nu}_\psi^+(u + \rho_N^I)}{\overline{\nu}_\psi^+(\rho_N^I)} \right)' du. \end{aligned}$$

By Proposition 3.1 of Smith (1987), under Assumptions 2, 4, and the assumption that $\rho_N^I \to \infty$, we get, conditional on $\mathcal{C}$,

$$\frac{1}{\overline{\nu}_\psi^+(\rho_N^I)} \int_{\mathbb{R}} \left(\log \left(\frac{\psi^+(x)}{\rho_N^I} \right) \right)^k \mathbf{1}_{\{\psi^+(x) > \rho_N^I\}} \nu(x) dx = (\xi_I^+)^k \Gamma(k+1) + O\big(\tau_I^+(\rho_N^I)\big), \tag{G.6}$$

where $\Gamma(\cdot)$ is the gamma function.

Next, we show the consistency of $\widetilde{\xi_I}^+$. By Assumptions 2 and 4, for the M_N^{I+} defined in (G.1),

$$\frac{\mathbb{E}(M_N^{I+}|\mathcal{C})}{N\overline{\nu}_\psi^+(\rho_N^I)} = \frac{1}{N}\sum_{i=1}^N \mathbb{E}\Big(\int_0^1 \varphi_{it}^+ dt \Big| \mathcal{C}\Big), \tag{G.7}$$

$$\frac{Var(M_N^{I+}|\mathcal{C})}{N\overline{\nu}_\psi^+(\rho_N^I)} = \frac{1}{N}\sum_{i=1}^N \mathbb{E}\Big(\int_0^1 \varphi_{it}^+ dt \Big| \mathcal{C}\Big) = O(1). \tag{G.8}$$

By (G.7) and (G.8), and the assumption that $N\overline{\nu}_\psi^+(\rho_N^I) \to \infty$ as $N \to \infty$, we have

$$\frac{M_N^{I+}}{N\overline{\nu}_\psi^+(\rho_N^I)} - \frac{1}{N}\sum_{i=1}^N \mathbb{E}\Big(\int_0^1 \varphi_{it}^+ dt \Big| \mathcal{C}\Big) = O_p\left(\sqrt{\frac{1}{N\overline{\nu}_\psi^+(\rho_N^I)}}\right) = o_p(1). \tag{G.9}$$

Similarly, using (G.6) with $k = 1$, we get

$$\begin{aligned} &\frac{1}{N\overline{\nu}_\psi^+(\rho_N^I)}\mathbb{E}\left(\sum_{i=1}^N \int_0^1 \int_{\mathbb{R}} \log\Big(\frac{\psi^+(x)}{\rho_N^I}\Big)\mathbf{1}_{\{\psi^+(x)>\rho_N^I\}}\mu_i(ds,dx)\right) \\ =&\Big((\xi_I^+) + O\big(\tau_I^+(\rho_N^I)\big)\Big)\left(\frac{1}{N}\sum_{i=1}^N \mathbb{E}\Big(\int_0^1 \varphi_{it}^+ dt\Big|\mathcal{C}\Big)\right), \end{aligned} \tag{G.10}$$

and by setting $k = 2$,

$$\begin{aligned} &\frac{1}{N\overline{\nu}_\psi^+(\rho_N^I)} Var\left(\sum_{i=1}^N \int_0^1 \int_{\mathbb{R}} \log\Big(\frac{\psi^+(x)}{\rho_N^I}\Big)\mathbf{1}_{\{\psi^+(x)>\rho_N^I\}}\mu_i(ds,dx)\Big|\mathcal{C}\right) \\ =&\frac{1}{N\overline{\nu}_\psi^+(\rho_N^I)}\sum_{i=1}^N Var\left(\int_0^1 \int_{\mathbb{R}} \log\Big(\frac{\psi^+(x)}{\rho_N^I}\Big)\mathbf{1}_{\{\psi^+(x)>\rho_N^I\}}\mu_i(ds,dx)\Big|\mathcal{C}\right) \\ =&\Big((\xi_I^+)^2 + O\big(\tau_I^+(\rho_N^I)\big)\Big)\left(\frac{1}{N}\sum_{i=1}^N \mathbb{E}\Big(\int_0^1 \varphi_{it}^+ dt\Big|\mathcal{C}\Big)\right) \\ =&O(1). \end{aligned} \tag{G.11}$$

By (G.10) and (G.11), $N\overline{\nu}_{\psi}^{+}(\rho_N^I) \to \infty$, and $\tau_I^+(\rho_N^I) = o(1)$, as $N \to \infty$, we have

$$\begin{aligned}
&\frac{1}{N\overline{\nu}_{\psi}^{+}(\rho_N^I)}\left(\sum_{i=1}^{N}\int_0^1\int_{\mathbb{R}}\log\Big(\frac{\psi^+(x)}{\rho_N^I}\Big)\mathbf{1}_{\{\psi^+(x)>\rho_N^I\}}\mu_i(ds,dx)\right)\\
&\qquad\qquad - \xi_I^+\left(\frac{1}{N}\sum_{i=1}^{N}\int_0^1\mathbb{E}(\varphi_{it}^+|\mathcal{C})dt\right) \qquad \text{(G.12)}\\
=&O_p\left(\sqrt{\frac{1}{N\overline{\nu}_{\psi}^{+}(\rho_N^I)}}+\tau_I^+(\rho_N^I)\right)=o_p(1).
\end{aligned}$$

Combining (G.9) and (G.12) yields

$$\widetilde{\xi}_I^+ - \xi_I^+ = o_p(1). \qquad \text{(G.13)}$$

Finally, about the CLT, we have the following. For some $0 < \iota < 1$, there exists $\mathcal{C}$-adapted positive random variable C such that

$$\begin{aligned}
&\mathbb{E}\left(\Big(\int_0^1\int_{\mathbb{R}}\log\Big(\frac{\psi^+(x)}{\rho_N^I}\Big)\mathbf{1}_{\{\psi^+(x)>\rho_N^I\}}\mu_i(ds,dx)\Big)^{2(1+\iota)}\Big|\mathcal{C}\right)\\
\le& C\mathbb{E}\left(\Big(\int_0^1\int_{\mathbb{R}}\log\Big(\frac{\psi^+(x)}{\rho_N^I}\Big)\mathbf{1}_{\{\psi^+(x)>\rho_N^I\}}\tilde{\mu}_i(ds,dx)\Big)^{2(1+\iota)}\Big|\mathcal{C}\right)\\
&+C\mathbb{E}\left(\Big(\int_0^1\varphi_{is}^+\int_{\mathbb{R}}\log\Big(\frac{\psi^+(x)}{\rho_N^I}\Big)\mathbf{1}_{\{\psi^+(x)>\rho_N^I\}}\nu_s(x)dsdx\Big)^{2(1+\iota)}\Big|\mathcal{C}\right) \qquad \text{(G.14)}\\
\le& C\mathbb{E}\left(\Big(\int_0^1\int_{\mathbb{R}}\log\Big(\frac{\psi^+(x)}{\rho_N^I}\Big)\mathbf{1}_{\{\psi^+(x)>\rho_N^I\}}\tilde{\mu}_i(ds,dx)\Big)^{2(1+\iota)}\Big|\mathcal{C}\right)\\
&+C\mathbb{E}\Big(\int_0^1(\varphi_{is}^+)^{2(1+\iota)}ds\Big|\mathcal{C}\Big)\Big(\overline{\nu}_{\psi}^{+}(\rho_N^I)\big(\xi_I^+ + O(\tau_I^+(\rho_N^I))\big)\Big)^{2(1+\iota)},
\end{aligned}$$

where $\tilde{\mu}_i(dt,dx) = \mu_i(dt,dx) - \nu_{it}(dx)dt$, and the last inequality holds due to the assumption that $\mathbb{E}((\varphi_{it}^+)^{2(1+\iota)}|\mathcal{C})$ is bounded by a $\mathcal{C}$-adapted random variable, Jensen's

inequality, (G.6) with $k=1$. By the Burkholder-Davis-Gundy inequality,

$$\begin{aligned}
&\mathbb{E}\bigg(\Big(\int_0^1\int_{\mathbb{R}}\log\Big(\frac{\psi^+(x)}{\rho_N^I}\Big)\mathbf{1}_{\{\psi^+(x)>\rho_N^I\}}\tilde{\mu}_i(ds,dx)\Big)^{2(1+\iota)}\bigg|\mathcal{C}\bigg)\\
\leq&\mathbb{E}\bigg(\Big(\int_0^1\int_{\mathbb{R}}\Big(\log\Big(\frac{\psi^+(x)}{\rho_N^I}\Big)\Big)^2\mathbf{1}_{\{\psi^+(x)>\rho_N^I\}}\mu_i(ds,dx)\Big)^{(1+\iota)}\bigg|\mathcal{C}\bigg)\\
\leq&C\mathbb{E}\bigg(\Big(\int_0^1\int_{\mathbb{R}}\Big(\log\Big(\frac{\psi^+(x)}{\rho_N^I}\Big)\Big)^2\mathbf{1}_{\{\psi^+(x)>\rho_N^I\}}\tilde{\mu}_i(ds,dx)\Big)^{(1+\iota)}\bigg|\mathcal{C}\bigg)\\
&+C\mathbb{E}\bigg(\Big(\int_0^1\int_{\mathbb{R}}\Big(\log\Big(\frac{\psi^+(x)}{\rho_N^I}\Big)\Big)^2\mathbf{1}_{\{\psi^+(x)>\rho_N^I\}}\varphi_{is}^+\nu_s(x)dsdx\Big)^{(1+\iota)}\bigg|\mathcal{C}\bigg).
\end{aligned}\tag{G.15}$$

For the first term on the right hand side of the last inequality of (G.15), by $\iota<1$, the inequality that $(\sum_i a_i)^p\leq\sum_i a_i^p$ for $p\leq 1$, and the Burkholder-Davis-Gundy inequality again, we have

$$\begin{aligned}
&\mathbb{E}\bigg(\Big(\int_0^1\int_{\mathbb{R}}\Big(\log\Big(\frac{\psi^+(x)}{\rho_N^I}\Big)\Big)^2\mathbf{1}_{\{\psi^+(x)>\rho_N^I\}}\tilde{\mu}_i(ds,dx)\Big)^{(1+\iota)}\bigg|\mathcal{C}\bigg)\\
\leq&\mathbb{E}\bigg(\Big(\int_0^1\int_{\mathbb{R}}\Big(\log\Big(\frac{\psi^+(x)}{\rho_N^I}\Big)\Big)^4\mathbf{1}_{\{\psi^+(x)>\rho_N^I\}}\mu_i(ds,dx)\Big)^{(1+\iota)/2}\bigg|\mathcal{C}\bigg)\\
\leq&\mathbb{E}\bigg(\int_0^1\int_{\mathbb{R}}\Big(\log\Big(\frac{\psi^+(x)}{\rho_N^I}\Big)\Big)^{2(1+\iota)}\mathbf{1}_{\{\psi^+(x)>\rho_N^I\}}\mu_i(ds,dx)\bigg|\mathcal{C}\bigg)\\
=&\mathbb{E}\Big(\int_0^1\int_{\mathbb{R}}\Big(\log\Big(\frac{\psi^+(x)}{\rho_N^I}\Big)\Big)^{2(1+\iota)}\mathbf{1}_{\{\psi^+(x)>\rho_N^I\}}\varphi_{is}^+\nu_s(x)dxds\bigg|\mathcal{C}\Big)\\
=&\Big(6(\xi_I^+)^4\overline{\nu}_\psi^+(\rho_N^I)+O(\tau_I^+(\rho_N^I))\Big)\mathbb{E}\Big(\int_0^1\varphi_{is}^+ds\bigg|\mathcal{C}\Big),
\end{aligned}\tag{G.16}$$

where the last equality holds by (G.6) with $k=4$.

For the second term on the right hand side of the last inequality of (G.15), by

(G.6) with $k=2$, we have, for some $\mathcal{C}$-adapted positive random variable C,

$$\begin{aligned}
&\mathbb{E}\left(\left(\int_0^1\int_{\mathbb{R}}\left(\log\left(\frac{\psi^+(x)}{\rho_N^I}\right)\right)^2\mathbf{1}_{\{\psi^+(x)>\rho_N^I\}}\varphi_{is}^+\nu_s(x)dxds\right)^{(1+\iota)}\middle|\mathcal{C}\right)\\
=&\mathbb{E}\left(\left(\int_0^1\varphi_{is}^+ds\left(\overline{\nu}_\psi^+(\rho_N^I)2(\xi_I^+)^2+O(\tau_I^+(\rho_N^I))\right)\right)^{(1+\iota)}\middle|\mathcal{C}\right)\\
\leq&C\mathbb{E}\left(\int_0^1(\varphi_{is}^+)^{1+\iota}ds\middle|\mathcal{C}\right)\left(\overline{\nu}_\psi^+(\rho_N^I)2(\xi_I^+)^2+O(\tau_I^+(\rho_N^I))\right)^{1+\iota},
\end{aligned}\tag{G.17}$$

where the last inequality holds by $\mathbb{E}\big((\varphi_{it}^+)^{(1+\iota)}|\mathcal{C}\big)$ being bounded by $\mathcal{C}$-adapted random variable and Jensen's inequality. Combining (G.14)–(G.17), the assumption that $\rho_N^I\to\infty$ hence $\overline{\nu}_\psi^+(\rho_N^I)\to 0$, and $N\overline{\nu}_\psi^+(\rho_N^I)\to\infty$ yields

$$\begin{aligned}
&\sum_{i=1}^N\frac{1}{N^{1+\iota}\big(\overline{\nu}_\psi^+(\rho_N^I)\big)^{1+\iota}}\mathbb{E}\left(\left(\int_0^1\int_{\mathbb{R}}\log\left(\frac{\psi(x)}{\rho_N^I}\right)\mathbf{1}_{\{\psi^+(x)>\rho_N^I\}}\mu_i(ds,dx)\right)^{2(1+\iota)}\middle|\mathcal{C}\right)\\
=&O\left(\frac{1}{N^\iota\big(\overline{\nu}_\psi^+(\rho_N^I)\big)^\iota}\right)\to 0 \text{ as } N\to\infty.
\end{aligned}\tag{G.18}$$

The desired result follows from (G.9), (G.10), (G.11), (G.18), the assumptions that $\sqrt{N\overline{\nu}_\psi^+(\rho_N^I)}\big(\tau_I^+(\rho_N^I)\big)=o(1)$, and Lyapunov's CLT. □

Next, for the infeasible estimator of the tail index of the systematic jumps, we have the following lemma.

Lemma 2 *For the process $\{p_{it}\}$ defined in (2.1), assume Assumptions 1–3, in addition, $N\to\infty$, $\rho_N^S\to\infty$, $\inf_{p\geq 1}N\overline{f}_{p,\psi}^+(\rho_N^S)\to\infty$, and $\sup_{p\geq 1}\sqrt{N\overline{f}_{p,\psi}^+(\rho_N^S)}\tau_S^+(\rho_N^S)\to 0$ as $N\to\infty$. Then*

$$\sqrt{M_N^{S+}}(\widetilde{\xi}_S^+-\xi_S^+)\overset{\mathcal{L}|\mathcal{C}}{\to}N\big(0,(\xi_S^+)^2\big).\tag{G.19}$$

Proof: By Proposition 3.1 of Smith (1987), under Assumptions 2, 3, and that $\rho_N^S\to\infty$, we get, for all $p\geq 1$,

$$\frac{1}{\overline{f}_{p,\psi}^+(\rho_N^S)}\mathbb{E}\left(\left(\log\left(\frac{\psi(\lambda_{ip})}{\rho_N^S}\right)\right)^k\mathbf{1}_{\{\psi(\lambda_{ip})>\rho_N^S\}}\middle|\mathcal{C}\right)=(\xi_S^+)^k\Gamma(k+1)+O\big(\tau_S^+(\rho_N^S)\big),\tag{G.20}$$

where $\Gamma(\cdot)$ is the gamma function. By Assumptions 1–3, for the M_N^{S+} defined in

(G.4),

$$\mathbb{E}(M_N^{S+}|\mathcal{C}) = \frac{N}{|T_n|}\sum_{p=1}^{T_n}\overline{f}_{p,\psi}^{+}(\rho_N^S), \tag{G.21}$$

$$Var(M_N^{S+}|\mathcal{C}) = \frac{N}{|T_n|}\sum_{p=1}^{T_n}\overline{f}_{p,\psi}^{+}(\rho_N^S). \tag{G.22}$$

Denote by $\overline{f}_{\psi}^{+}(\rho_N^S) = \sum_{p=1}^{T_n}\overline{f}_{p,\psi}^{+}(\rho_N^S)/|T_n|$. By (G.21) and (G.22), and the assumption that $\inf_{p\geq 1} N\overline{f}_{\psi}^{+}(\rho_N^S) \to \infty$ as $N \to \infty$, we have $N\overline{f}_{\psi}^{+}(\rho_N^S) \to \infty$, and

$$\frac{M_N^{S+}}{N\overline{f}_{\psi}^{+}(\rho_N^S)} - 1 = O_p\left(\sqrt{\frac{1}{N\overline{f}_{\psi}^{+}(\rho_N^S)}}\right) = o_p(1). \tag{G.23}$$

Using (G.20) with $k = 1$, we get

$$\frac{1}{N\overline{f}_{\psi}^{+}(\rho_N^S)}\mathbb{E}\left(\sum_{i=1}^{N}\sum_{p\geq 1}\lambda_{ip}\mathbf{1}_{\{\psi^+(\lambda_{ip})>\rho_N^S\}}\middle|\mathcal{C}\right) = \xi_S^+ + O\big(\tau_S^+(\rho_N^S)\big), \tag{G.24}$$

and by setting $k = 2$,

$$\begin{aligned}
&\frac{1}{N\overline{f}_{\psi}^{+}(\rho_N^S)}Var\left(\sum_{i=1}^{N}\sum_{p\geq 1}\log\left(\frac{\psi^+(\lambda_{ip})}{\rho_N^S}\right)\mathbf{1}_{\{\psi^+(\lambda_{ip})>\rho_N^S\}}\middle|\mathcal{C}\right)\\
=&\frac{1}{N\overline{f}_{\psi}^{+}(\rho_N^S)}\sum_{i=1}^{N}Var\left(\sum_{p\geq 1}\log\left(\frac{\psi^+(\lambda_{ip})}{\rho_N^S}\right)\mathbf{1}_{\{\psi^+(\lambda_{ip})>\rho_N^S\}}\middle|\mathcal{C}\right)\\
=&(\xi_S^+)^2 + O\big(\tau_S^+(\rho_N^S)\big)\\
=&O_p(1).
\end{aligned} \tag{G.25}$$

By (G.24) and (G.25), $N\overline{f}_{\psi}^{+}(\rho_N^S) \to \infty$, and $\tau_S^+(\rho_N^S) = o(1)$ as $N \to \infty$, we have

$$\begin{aligned}
&\frac{1}{N\overline{f}_{\psi}^{+}(\rho_N^S)}\left(\sum_{i=1}^{N}\sum_{p\geq 1}\log\left(\frac{\psi^+(\lambda_{ip})}{\rho_N^S}\right)\mathbf{1}_{\{\psi^+(\lambda_{ip})>\rho_N^S\}}\right) - \xi_S^+\\
=&O_p\left(\sqrt{\frac{1}{N\overline{f}_{\psi}^{+}(\rho_N^S)}} + \tau_S^+(\rho_N^S)\right) = o_p(1).
\end{aligned} \tag{G.26}$$

By (G.23) and (G.26), we get

$$\widetilde{\xi}_S^+ - \xi_S = o_p(1). \tag{G.27}$$

Finally, to show the CLT, by (G.20) with $k = 4$, we have

$$\begin{aligned}
&\frac{1}{N^2\big(\overline{f}_\psi^+(\rho_N^S)\big)^2}\sum_{i=1}^N\sum_{p\geq 1}\mathbb{E}\left(\log\left(\frac{\psi^+(\lambda_{ip})}{\rho_N^S}\right)\mathbf{1}_{\{\psi^+(\lambda_{ip})>\rho_N^S\}}\right)^4\Big|\mathcal{C}\Big) \\
=&\frac{|T_n|}{N\big(\overline{f}_\psi^+(\rho_N^S)\big)^2}\Big(6(\xi_S^+)^4\overline{f}_\psi^+(\rho_N^S) + O_p(\tau_S^+(\rho_N^S))\Big) \\
=&O_p\left(\frac{1}{N\overline{f}_\psi^+(\rho_N^S)}\right) \to 0 \text{ as } N\to\infty,
\end{aligned} \tag{G.28}$$

where the last line holds by the assumptions that $\inf_{p\geq 1} N\overline{f}_{p,\psi}^+(\rho_N^S) \to \infty$, and $\sup_{p\geq 1}\sqrt{N\overline{f}_{p,\psi}^+(\rho_N^S)}\big(\tau_S^+(\rho_N^S)\big) = o(1)$, which implies that $\sqrt{N\overline{f}_\psi^+(\rho_N^S)}\big(\tau_S^+(\rho_N^S)\big) = o(1)$, and $N\overline{f}_\psi^+(\rho_N^S)\to\infty$. The desired result then follows from (G.23), (G.24), (G.25), (G.28), $\sqrt{N\overline{f}_\psi^+(\rho_N^S)}\big(\tau_S^+(\rho_N^S)\big) = o(1)$, $N\overline{f}_\psi^+(\rho_N^S)\to\infty$, and Lyapunov's CLT. □

The following two lemmas are about comparing the feasible with infeasible estimators of the jump tail indices.

Lemma 3 *Assume that Assumptions 1, 2, 4 and 5 hold, $\nu(x)$ is nonincreasing for x sufficiently large. Let $\rho_N > 1$ be a deterministic sequence as a function of the dimension N, such that $\rho_N \uparrow \infty$ as $N\uparrow\infty$. In addition, $N\overline{\nu}^+(\log(\rho_N))\to\infty$,*

$$\sqrt{N\overline{\nu}^+(\log(\rho_N))\Delta_n^{1-\varepsilon}}\left(1\bigvee\frac{\sqrt{\Delta_n}}{\overline{\nu}^+(\log(\rho_N))}\right)\to 0 \text{ as } N\uparrow\infty, \Delta_n\downarrow 0,$$

where $\overline{\nu}^+(x) = \int_x^\infty \nu(z)dz$. We consider the following class of functions $\mathcal{G} = \{g_N(\cdot)\}$ that satisfies for $g_N(x)\in\mathcal{G}$:

(a) $g_N(x) = 0$ for $x < \log(\rho_N)$,

(b) $|g_N(x)| \leq C(x - \log(\rho_N))$ and $|g_N'(x)|\leq C$ for $x\geq\log(\rho_N)$, where $g_N'(\rho_N)$ is the right derivative.

Then, as $N \uparrow \infty, \Delta_n \downarrow 0$,

$$\sup_{g\in\mathcal{G}} \frac{1}{\sqrt{N\overline{\nu}^+(\log(\rho_N))}} \left(\sum_{i=1}^{N} \sum_{j\in T_n^c} g_N(\Delta_j^n p_i) - \sum_{i=1}^{N} \sum_{0\le s\le 1, s\notin\{\rho_p\}_{p\ge 1}} g_N(\Delta p_{is}) \right) \xrightarrow{P} 0, \tag{G.29}$$

where $\Delta p_{is} = p_{is} - p_{is-}$ *for* $i = 1, ..., N$.

Proof: Under Assumption 5, we have for all $i \ge 1$, $q \ge 2$ and $\varepsilon > 0$,

$$\begin{aligned} & P(\sup_{u\in[0,1]} \varphi_{iu}^+ \ge \Delta_n^{-\varepsilon} | \mathcal{C}) \\ \le & P(\sup_{u\in[0,1]} |\varphi_{iu}^+ - \varphi_{i0}^+| \ge \Delta_n^{-\varepsilon}/2 | \mathcal{C}) + P(\varphi_{i0}^+ \ge \Delta_n^{-\varepsilon}/2 | \mathcal{C}) \\ \le & K_q \Delta_n^{q\varepsilon}. \end{aligned} \tag{G.30}$$

The rest of the proof is identical to steps 2–11 in the proof of Lemma 3 of Bollerslev and Todorov (2011) by replacing T therein by N. Details are hence omitted. □

Lemma 4 *Assume that Assumptions 1–5 hold,* $\nu(x)$ *is nonincreasing for* x *sufficiently large. Let* $\rho_N > 1$ *be a deterministic sequence as a function of the dimension* N, *such that* $\rho_N \uparrow \infty$ *as* $N \uparrow \infty$. *In addition,* $\inf_{p\ge 1} N\overline{f}_{p,\psi^+}(\rho_N) \to \infty$, $\sup_{p\ge 1} \Delta_n \overline{\nu}_{\psi}^+(\rho_N) \sqrt{N/\overline{f}_{p,\psi^+}(\rho_N)} \to 0$, *and for some* $\varepsilon \in (0,1)$, *as* $N \uparrow \infty, \Delta_n \downarrow 0$,

$$\sup_{p\ge 1} \sqrt{N\overline{f}_p^+(\log(\rho_N))\Delta_n^{3-\varepsilon}} \left(1 \bigvee \frac{\sqrt{\Delta_n}}{\inf_{p\ge 1} \overline{f}_p^+(\log(\rho_N))} \right) \to 0, \tag{G.31}$$

where $\overline{\nu}^+(x) = \int_x^\infty \nu(z)dz$, *and* $\overline{f}^+(x) = \int_x^\infty f(z)dz$. *Then we have, for the function class* $\mathcal{G}$ *defined in Lemma 3, as* $N \uparrow \infty, \Delta_n \downarrow 0$,

$$\sup_{g\in\mathcal{G}} \frac{1}{\sqrt{N\overline{f}^+(\log(\rho_N))}} \left(\sum_{i=1}^{N} \sum_{j\in T_n} g_N(\Delta_j^n p_i) - \sum_{i=1}^{N} \sum_{p\ge 1} g_N(\Delta p_{i\rho_p}) \right) \xrightarrow{P} 0, \tag{G.32}$$

where $\overline{f}^+(\log(\rho_N)) = \sum_{p=1}^{|T_n|} \overline{f}_p^+(\log(\rho_N))/|T_n|$.

Proof: By (G.30), Assumption 1, and replacing T in steps 2–11 in the proof of Lemma 3 of Bollerslev and Todorov (2011) by $N\Delta_n$, one can show that under the

condition (G.31),

$$\sup_{g\in\mathcal{G}}\frac{1}{\sqrt{N\overline{f}^{+}(\log(\rho_N))}}\Bigg(\sum_{i=1}^{N}\sum_{j\in T_n}g_N(\Delta_j^n p_i)-\sum_{i=1}^{N}\sum_{\lfloor(s\Delta_n)\rfloor\in T_n,s\notin\{\rho_p\}_{p\geq1}}g_N(\Delta p_{is})$$
$$-\sum_{i=1}^{N}\sum_{p\geq1}g_N(\Delta p_{i\rho_p})\Bigg)\xrightarrow{P}0.$$

Under the assumption that $\sup_{p\geq1}\Delta_n\overline{\nu}_{\psi}^{+}(\rho_N)\sqrt{N/\overline{f}_{p,\psi^+}(\rho_N)}\to0$, by Lemma 1, we have

$$\begin{aligned}&\sup_{g\in\mathcal{G}}\sum_{i=1}^{N}\sum_{\lfloor(s\Delta_n)\rfloor\in T_n,s\notin\{\rho_p\}_{p\geq1}}g_N(\Delta p_{is})\\&=O_p\Big(N\overline{\nu}^{+}(\log(\rho_N))\Delta_n+\sqrt{N\overline{\nu}^{+}(\log(\rho_N))\Delta_n}\Big)\\&=o_p\Big(\sqrt{N\overline{f}^{+}(\log(\rho_N))}\Big).\end{aligned}$$

From here, the desired conclusion follows. □

Proof of Theorem 1:

By Lemma 3 with $g(x)=\mathbf{1}_{\{\psi(x)\geq\rho_N\}}$, and $g(x)=(\log(\psi(x))-\log(\rho_N))\mathbf{1}_{\{\psi(x)\geq(\rho_N)\}}$, under Assumption 1, we get that

$$\widehat{M}_N^{S+}-M_N^{S+}=o_p(\sqrt{N\overline{f}_{\psi}^{+}(\rho_N^S)}),\tag{G.33}$$

and

$$\begin{aligned}&\sum_{i=1}^{N}\sum_{j=1}^{\hat{T}_n}\log\Big(\frac{\psi^+(\Delta_j^n p_i)}{\rho_N^S}\Big)\mathbf{1}_{\{\psi^+(\Delta_j^n p_i)>\rho_N^S\}}\\&\qquad-\sum_{i=1}^{N}\sum_{p\geq1}\log\Big(\frac{\psi^+(\lambda_{ip})}{\rho_N^S}\Big)\mathbf{1}_{\{\psi^+(\lambda_{ip})>\rho_N^S\}}\\&=o_p\Big(\sqrt{N\overline{f}^{+}(\log(\rho_N^S))}\Big).\end{aligned}\tag{G.34}$$

The desired result then follows from (G.23), (G.33), (G.34), Assumption 1 and Lemma 2. □

Proof of Theorem 2:

By Lemma 3 with $g(x)=\mathbf{1}_{\{\psi(x)\geq\rho_N\}}$, and $g(x)=(\log(\psi(x))-\log(\rho_N))\mathbf{1}_{\{\psi(x)\geq(\rho_N)\}}$,

we get that

$$\widehat{M}_N^{I+} - M_N^{I+} = o_p\Big(\sqrt{N\overline{\nu}_\psi^+(\rho_N^I)}\Big), \tag{G.35}$$

and

$$\begin{aligned}
&\sum_{i=1}^{N}\sum_{j=1}^{n}\log\Big(\frac{\psi^+(\Delta_j^n p_i)}{\rho_N^I}\Big)\mathbf{1}_{\{\psi^+(\Delta_j^n p_i)>\rho_N^I\}} \\
&\quad -\sum_{i=1}^{N}\int_0^1\int_{\mathbb{R}}\log\Big(\frac{\psi^+(x)}{\rho_N^I}\Big)\mathbf{1}_{\{\psi^+(x)>\rho_N^I\}}\mu_i(ds,dx) \\
=&o_p\Big(\sqrt{N\overline{\nu}^+(\log(\rho_N^I))}\Big).
\end{aligned} \tag{G.36}$$

The desired result then follows from (G.9), (G.35), (G.36), Assumption 1 and Lemma 1.□

Next, we present the proof of Theorem 4 with Theorem 3 being shown in a similar way.

Proof of Theorem 4: By the triangle inequality,

$$|D_N^{I+} - \tilde{D}_N^{I+}| \le \sup_x |F_N^{I+}(x) - \tilde{F}_N^{I+}(x)| + \sup_x |P_N^{I+}(x) - \tilde{P}_N^{I+}(x)|, \tag{G.37}$$

where $\tilde{F}_N^{I+}(x)$ is the empirical tail distribution of the idiosyncratic jumps, $\tilde{P}_N^{I+}(x)$ is the corresponding Pareto tail probability with estimated tail index $\widetilde{\xi}_I^+$, and $\tilde{D}_N^I$ is the KS statistic computed using the infeasible idiosyncratic jumps, that is,

$$\tilde{F}_N^{I+}(x) = \frac{1}{M_N^{I+}}\sum_{i=1}^{N}\sum_{s\in[0,1],s\notin\{\rho_p\}_{p\ge1}}\mathbf{1}_{\{\psi(\Delta p_{is})>x\}} \quad \text{for } x \ge \rho_N^I,$$

$$\tilde{P}_N^{I+}(x) = \left(\frac{x}{M_N^{I+}}\right)^{-1/\widetilde{\xi}_I^+} \quad \text{for } x \ge \rho_N^I,$$

and

$$\tilde{D}_N^{I+} = \sup_x |\tilde{F}_N^{I+}(x) - \tilde{P}_N^{I+}(x)|.$$

By (G.35) and (G.36), we have

$$\sqrt{M_N^{I+}}(\sup_x |P_N^{I+}(x) - \tilde{P}_N^{I+}(x)|) = o_p(1). \tag{G.38}$$

By Assumption 4, $\tau_I^+(x) \equiv 0$ for all $x \geq \rho_N^I$, and (G.9),

$$\sqrt{M_N^{I+}}\widetilde{D}_N^{I+} \xrightarrow{\mathcal{L}} \mathcal{K}^{I+}. \tag{G.39}$$

We will show that

$$\sup_x |F_N^{I+}(x) - \tilde{F}_N^{I+}(x)| = o_p\left(\sqrt{\frac{1}{M_N^{I+}}}\right). \tag{G.40}$$

The desired result in Theorem 4 will then follow from (G.35), (G.37), (G.38), (G.39), and (G.40).

It remains to show (G.40). We choose a grids of x's, $0 = x_0 \leq x_1 \leq x_2, ..., \leq x_K$. Let $x_1 = \rho_N^I$, $F_N^{I+}(x_K) = o(\sqrt{N\overline{\nu}_\psi^+(\rho_N^I)})$, $K \gg \sqrt{N\overline{\nu}_\psi^+(\rho_N^I)}$, and we set the x_i's satisfy

$$\sup_{1\leq i\leq K} F_N^{I+}(x_i) - F_N^{I+}(x_{i-1}) = o\left(\sqrt{\frac{1}{N\overline{\nu}_\psi^+(\rho_N^I)}}\right). \tag{G.41}$$

By Lemma 3,

$$\sup_{x\in\{x_0,x_1,...,x_K\}} |F_{N,t}^{I+}(x) - \tilde{F}_{N,t}^{I+}(x)| = o_p\left(\sqrt{\frac{1}{M_N^{I+}}}\right). \tag{G.42}$$

In addition, for any $x \geq \rho_N^I$, there exists $x_i \leq x \leq x_{i+1}$ for some integer $i \geq 0$. We have

$$\begin{aligned} F_{N,t}^{I+}(x) - \tilde{F}_{N,t}^{I+}(x) &\leq F_{N,t}^{I+}(x_{i+1}) - \tilde{F}_{N,t}^{I+}(x_i) \\ &\leq F_{N,t}^{I+}(x_{i+1}) - F_{N,t}^{I+}(x_i) + |F_{N,t}^{I+}(x_i) - \tilde{F}_{N,t}^{I+}(x_i)|, \end{aligned}$$

and

$$\begin{aligned} F_{N,t}^{I+}(x) - \tilde{F}_{N,t}^{I+}(x) &\geq F_{N,t}^{I+}(x_i) - \tilde{F}_{N,t}^{I+}(x_{i+1}) \\ &\geq -\left(|F_{N,t}^{I+}(x_{i+1}) - F_{N,t}^{I+}(x_i)| + |F_{N,t}^{I+}(x_i) - \tilde{F}_{N,t}^{I+}(x_i)|\right). \end{aligned}$$

Therefore

$$\sup_x |F_{N,t}^{I+}(x) - \tilde{F}_{N,t}^{I+}(x)| \leq \sup_{0\leq i\leq K} |F_{N,t}^{I+}(x_{i+1}) - F_{N,t}^{I+}(x_i)| + \sup_{0\leq i\leq K} |F_{N,t}^{I+}(x_i) - \tilde{F}_{N,t}^{I+}(x_i)|.$$

The desired bound (G.40) then follows from (G.41) and (G.42). □